UNITED STATES AIR FORCE

AIR UNIVERSITY

AIR FORCE INSTITUTE OF TECHNOLOGY

Wright-Patterson Air Force Base, Ohio

AFIT/GAE/AA/78D-1

LEVEL II

A STUDY OF THE USE OF LAMINATED COMPOSITE WING STRUCTURES FOR CONTROLLING THE DIVERGENCE SPEED OF FORWARD SWEPT WINGS

THESIS

AFIT/GAE/AA/78D-1

David C. Bannerman
2nd Lt USAF

Approved for public release; distribution unlimited.

(14) AFIT/GAE/AA/78D-1

(6) A STUDY OF THE USE OF LAMINATED COMPOSITE WING STRUCTURES FOR CONTROLLING THE DIVERGENCE SPEED OF FORWARD SWEPT WINGS

(9) Master's THESIS

Presented to the Faculty of the School of Engineering
of the Air Force Institute of Technology
Air University (ATC)
in Partial Fulfillment of the
Requirements for the Degree of
Master of Science

(12) 76

(10) by

David C. Bannerman, B.S.
2nd Lt USAF
Graduate Aerospace Engineering

(11) Dec [redacted] 78

Approved for public release; distribution unlimited.

Preface

I would like to thank my advisor, Dr. Franklin E. Eastep for his special help and guidance on this thesis. His class lectures and timely remarks proved to be invaluable. I also wish to thank Dr. Vipperla B. Venkayya for his critical suggestions and advice.

I also wish to thank my wife, Karen, and my son, Crispin, for their relentless patience, forbearance, and thoughtfulness in helping me through the critical phases of this thesis.

David C. Bannerman

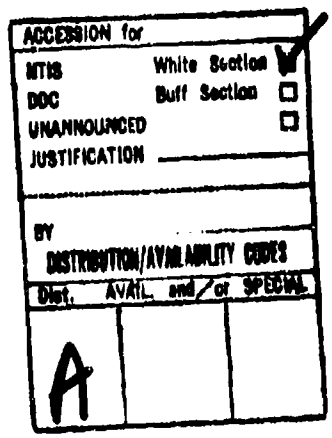

Contents

List of Figures

List of Symbols

A	cross sectional area of a rod
$A_{i,j}$	aerodynamic matrix coefficient
C	generalized flexibility influence coefficient
$C_{i,j}$	flexibility matrix coefficient
D_j	drag force
E	modulus of elasticity
$\bar{F}$	generalized applied force
F_x, F_y, F_z	applied forces in the x, y, and z directions
k	generalized stiffness influence coefficient
$k_{i,j}$ $K_{i,j}$	elemental and structural stiffness matrix coefficients
k_{rod}	stiffness matrix for a rod element
L	length of a rod
L	total lift for a wing
L_j, L_j	lift per unit span and total lift for the j^{th} aerodynamic panel
M_x, M_{x_o}, M_y, M_{y_o}, M_z	applied moments about the x, x_o, y, y_o, and Z axis
N	number of upper surface nodes and also the number of aerodynamic panels
S_j, S	span length of the j^{th} aerodynamic panel
U_∞	free stream velocity
U_{DIV}	free stream velocity for divergence
w	z component of free stream velocity
$\hat{x}, \hat{y}, \hat{z}$	displacement degrees of freedom
x, y, x_1, y_1	coordinate variables

x_i, y_i	coordinates of the i^{th} control point
x_j, y_j	coordinates of the j^{th} circulation singularity point
$\bar{x}$	$x_i - x_j$
$\bar{y}$	$y_i - y_j$
Z_a	equation of wing camber line
α, α_i	angle of attack
γ, Γ_j	circulation strength per unit area and per unit span
$\bar{\delta}, \delta_i$	generalized displacements
$\delta(t-t_o)$	Dirac delta function
θ	fiber orientation angle
θ_{eff}	effective nodal rotations
$\theta_x, \theta_y, \theta_z$	rotation degrees of freedom
λ	eigenvalue
Λ	wing sweep angle
ρ_∞	free stream density

Abstract

This thesis is an investigation of the effects of composite laminate orientation on the divergence problem of forward swept wings. The aerodynamic and structural properties are modeled with a doublet lattice technique and finite element method, respectively. The static equilibrium equation is applied to combine the two models. This results in an eigenvalue problem with the divergence dynamic pressure as the lowest eigenvalue.

A computer program is written to formulate and solve the eigenvalue problem. It is applied to two cases of example wings. For the first case, 100% of the fibers are varied from 0° to 50° ahead of the structural sweep axis for five different sweep angles. For the second case, only 70% of the fibers are varied while the remaining fibers are oriented at 90° and $\pm 45^{\circ}$ to the structural sweep axis.

The results indicate that the divergence problem can be effectively controlled and possibly eliminated by properly orienting the composite laminates. The divergence speed was found to increase and reach a maximum as the principal fiber direction is swept forward. Maximum values occur for fibers oriented between 15° and 20° ahead of the structural sweep axis for wings swept forward more than 25°.

A STUDY OF THE USE OF LAMINATED COMPOSITE WING STRUCTURES FOR CONTROLLING THE DIVERGENCE SPEED OF FORWARD SWEPT WINGS

I. Introduction

Background

The use of forward swept wings in aircraft design is practically nonexistant. This can be attributed to the aeroelastic phenomenon known as divergence. The divergence speed of a wing can be defined in the following manner:

> When a wing reaches its divergence speed, the increase of aerodynamic forces due to an arbitrary increase of the twist angle, is exactly equal to the increase of elastic restoring forces. When this speed is exceeded, the increase of elastic restoring forces required to counteract the increased aerodynamic forces, exceeds the elastic limits of the structure. This instability can result in drastic deformations and the destruction of the wing.

The excess structural weight of conventional metallic structures required to counteract divergence has been so great as to prohibit the use of forward swept wings. Since the divergence problem is practically nonexistant in conventional swept back designs, little has been learned on how to control divergence.

However, swept forward wings are aerodynamically superior to swept back designs. Several important advantages are discussed by both Krone (Ref 6) and Weisshaar (Ref 7). The reports published by these two men indicate that the divergence problem can be effectively eliminated by the proper use of advanced composite materials. In his report, Krone demonstrated that the use of composite materials for wing surfaces could control divergence without adding significant amounts of structural weight. Weisshaar combined aerodynamic strip theory with a simple box structure to predict that composite fiber orientations of 10° to 15° ahead of the structural sweep axis are the most effective in controlling divergence.

It is the purpose of this paper to continue the study of composite materials and their affect on the divergence speed of forward swept wings. An attempt will be made to verify the conclusions of Krone and Weisshaar using methods different from theirs.

Scope

An eigenvalue problem was developed to study the affects of composite fiber orientation on the divergence speed of forward swept wings. A doublet lattice method was used to model the aerodynamic forces. It represents the continuous lift distribution as a discrete set of forces dependent upon the rigid and elastic orientation of the wing. Similarly, the structural properties were modeled with a finite element method. The static equilibrium equation was used to relate the structural deformations to the externally applied forces. Combination of the two models results in an eigenvalue problem

with the divergence dynamic pressure as the lowest eigenvalue.

NASTRAN was used to determine the flexibility matrix for the structure. Another program combines NASTRAN's flexibility matrix with an aerodynamic matrix calculated from the doublet lattice method. It formulates the eigenvalue problem and solves it for the divergence speed. This program was applied to several example wings and the composite lamina orientations were varied. Divergence speeds were calculated and compared. Conclusions were made on how the divergence speed is affected by composite fiber orientation.

II. Formulatio of Method for Calculating Divergence Speed

Introduction

The development of the eigenvalue problem begins with the basic equilibrium equation:

$$\bar{F} = k\bar{\delta} \tag{1}$$

This equation relates the static aerodynamic forces (F) to the wing displacements (δ). The typical wing is a very complex structure consisting of many intricate structural members. Because of this it is all but impossible to develop an accurate analytic expression for the stiffness coefficient (k). The resultant fact is that the equilibrium equation is very difficult to apply in its present form. Also, several important variables are not present. The aerodynamic forces depend not only on the local angle of attack of the wing but also on the fluid velocity and density. None of these terms are evident in the equilibrium expression. If the equilibrium equation is written:

$$c\bar{F} = \bar{\delta} \tag{2}$$

where c is the flexibility influence coefficient, the displacements are seen to rely upon the applied forces as well as the complicated structure. It is evident that the equilibrium equation must be expanded and simplified.

The wing will be simplified by modeling it with a finite element model. This will discretize the wing and allow the equilibrium equation to be expressed in matrix form. Then a doublet lattice

aerodynamic method will be applied to determine the aerodynamic forces as functions of the local angles of attack of the different wing sections. This aerodynamic model will than be combined with the structural model so that the eigenvalue problem can be expressed by a single equation. The velocity at which the wing diverges will be the eigenvalue and the rotational displacements about the y-axis (local change in angle of attack) will become the eigenvector.

Structural Wing Model

The first step in developing a workable relation is to model the wing with a finite element model. The wing, which has an infinite number of degrees of freedom as a continuous structure, is modeled as a discrete set of points. At each of these points, or nodes, the structure is allowed to have six degrees of freedom, three displacements and three rotations. The nodes are located at key positions on the wing so that they can be connected with simple structural elements to approximate the actual structural members. Ribs and spars are replaced by a combination of rod and shear panel elements. Skin surfaces are replaced by membrane or thin plate elements. In this manner the entire structure is broken down into more workable elements. Figure 1 illustrates the finite element model and also defines the coordinate system used to define the structure and its degrees of freedom.

Analytical methods are applied to the individual elements to distribute an effective stiffness to its nodes. This is done so that when the elements are connected, their effective stiffness terms add to form a stiffness matrix for the entire wing structure. The

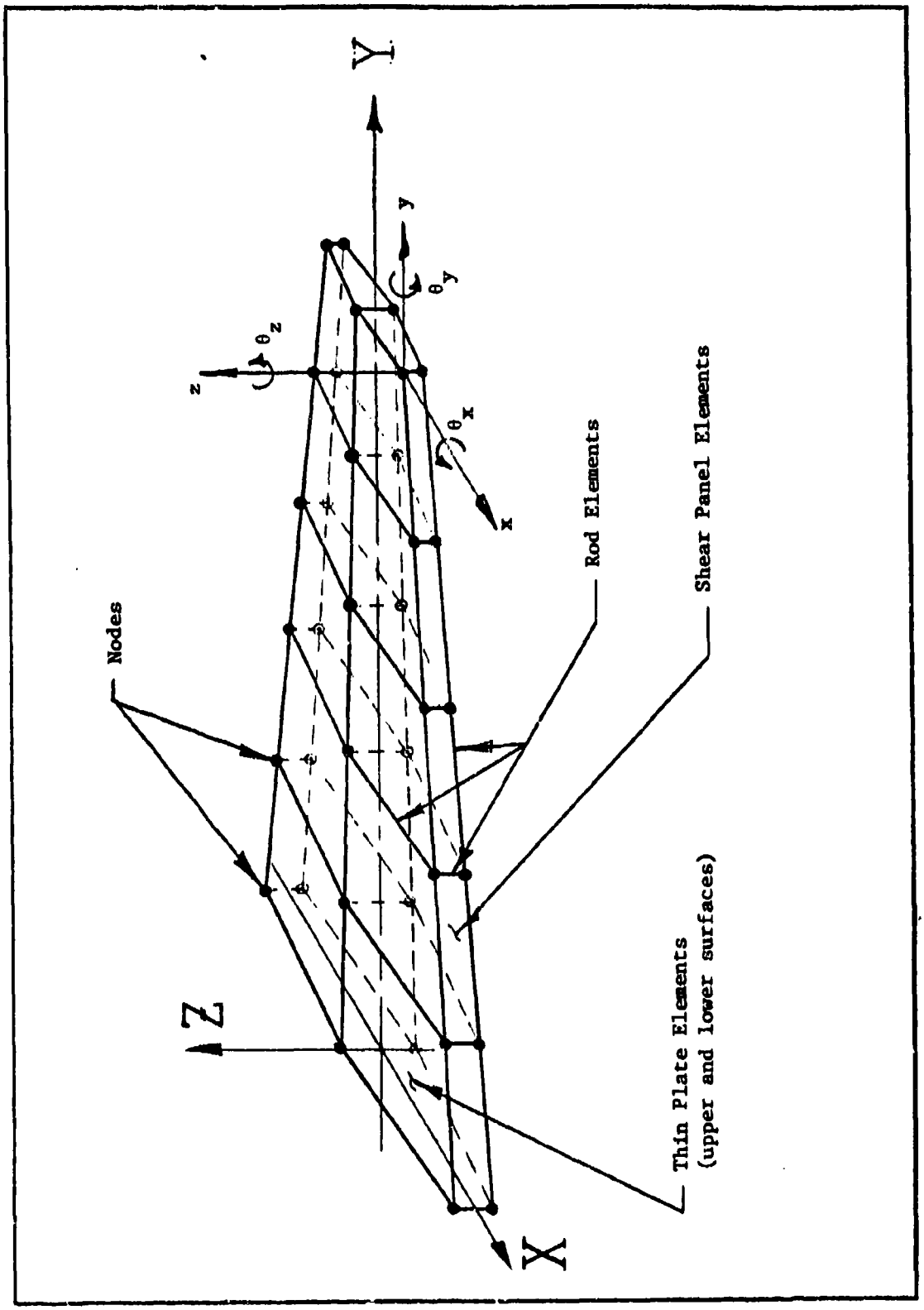

Figure 1. Finite Element Structural Model

stiffness matrix for both an element and the entire structure can be defined in the following manner:

> The elements k_{ij} of the stiffness matrix are the infinitesimal changes in the forces (F_i) required at the i^{th} nodes to infinitesimally change the displacement at the node j and hold all other displacements constant, i.e.

$$k_{ij} = \frac{\partial F_i}{\partial \delta_j}$$

The stiffness matrix will vary in shape and value from structure to structure, depending on the type and number of elements comprising the structure. However, the elemental stiffness matrices for each type of element always have the same form and only depend upon the material and geometrical properties of the element. For example, the rod element has the following stiffness matrix:

$$[k_{rod}] = \frac{EA}{L}\begin{bmatrix} 1 & -1 \\ -1 & 1 \end{bmatrix} \tag{3}$$

The only variables in this matrix are E, A, and L. They are the material and geometrical properties of the rod. Likewise, shear panel, plate, and membrane element matrices can be shown to depend upon only geometric and material properties. (The elemental stiffness matrices for these elements will not be reproduced here due to their complex form. References 5 and 6 contain a more detailed account of the development of the stiffness matrices and the finite element method in general.) Because of this dependence on only geometric and material properties, the finite element method can be readily programed into

a computer. There are many widely used programs that require only the appropriate geometric and material properties of the individual elements to assemble a stiffness matrix for the entire structure. Including the nodal forces might permit a detailed stress analysis to be made. One such program is NASTRAN.

NASTRAN was developed by NASA to analyze virtually any structure. A wide variety of structural elements, ranging from the simple bar element to the complicated quadrilateral plate element, can be used to analyze both static and dynamic problems. It has the capability to find stresses, displacements, natural modes, and natural frequencies and can also be applied to wing structures to calculate flutter speeds. NASTRAN is widely used within the aerospace industry for structural analysis.

Within the framework of this study, NASTRAN will be used to formulate the stiffness matrix for a test wing and calculate the appropriate flexibility matrix. This flexibility matrix is the inverse of the stiffness matrix. It can be found by either inverting the stiffness matrix or applying the following definition:

> C_{ji} . . . the i^{th} column of the flexibility matrix is a displacement configuration for the j^{th} nodes resulting from a force system of F_i = unity and all other nodal forces zero.

Flexibility influence coefficients are used quite often in aerodynamic analysis and will be used to represent the structure in this development of the eigenvalue problem.

The finite element model has effectively transformed the equilibrium equation to matrix form:

$$\{F_i\} = [K_{ij}]\{\delta_j\} \tag{4}$$

or

$$[C_{ji}]\{F_i\} = \{\delta_j\} \tag{5}$$

The flexibility matrix of Eq 5 can be partitioned in such a manner as to separate the different types of degrees of freedom. Likewise, the force and displacement vectors can be partitioned in a similar manner to produce:

$$\left[\begin{array}{c|c|c|c|c|c} C_{xx} & C_{xy} & C_{xz} & C_{x\theta_x} & C_{x\theta_y} & C_{x\theta_z} \\ \hline C_{yx} & C_{yy} & C_{yz} & C_{y\theta_x} & C_{y\theta_y} & C_{y\theta_z} \\ \hline C_{zx} & C_{zy} & C_{zz} & C_{z\theta_x} & C_{z\theta_y} & C_{z\theta_z} \\ \hline C_{\theta_x x} & C_{\theta_x y} & C_{\theta_x z} & C_{\theta_x\theta_x} & C_{\theta_x\theta_y} & C_{\theta_x\theta_z} \\ \hline C_{\theta_y x} & C_{\theta_y y} & C_{\theta_y z} & C_{\theta_y\theta_x} & C_{\theta_y\theta_y} & C_{\theta_y\theta_z} \\ \hline C_{\theta_z x} & C_{\theta_z y} & C_{\theta_z z} & C_{\theta_z\theta_x} & C_{\theta_z\theta_y} & C_{\theta_z\theta_z} \end{array}\right] \left\{\begin{array}{c} F_x \\ -- \\ F_y \\ -- \\ F_z \\ -- \\ M_x \\ -- \\ M_y \\ -- \\ M_z \end{array}\right\} = \left\{\begin{array}{c} \hat{x} \\ -- \\ \hat{y} \\ -- \\ \hat{z} \\ -- \\ \theta_x \\ -- \\ \theta_y \\ -- \\ \theta_z \end{array}\right\} \tag{6}$$

This system can be reduced and simplified further by making several important assumptions regarding the structure and the aerodynamic forces.

The first assumption is that the wing is sufficiently rigid in the X - Y plane so that the inplane displacements are small and can be neglected. This eliminates the x, y, and θ_z degrees of freedom.

Equation 6 is reduced to:

$$\begin{bmatrix} C_{zz} & C_{z\theta_x} & C_{z\theta_y} \\ C_{\theta_x z} & C_{\theta_x\theta_x} & C_{\theta_x\theta_y} \\ C_{\theta_y z} & C_{\theta_y\theta_x} & C_{\theta_y\theta_y} \end{bmatrix} \begin{Bmatrix} F_z \\ M_x \\ M_y \end{Bmatrix} = \begin{Bmatrix} \hat{z} \\ \theta_x \\ \theta_y \end{Bmatrix} \tag{7}$$

The second assumption is that the aerodynamic forces act as a distributed pressure over the upper surface of the wing. This allows the pressure to be represented by a finite set of forces acting only at the upper nodes, eliminating the lower nodes from the equilibrium equation. However, the entire structure will still be represented by the values of the remaining flexibility coefficients. The remaining forces in the x and y directions have already been eliminated with the previous assumption leaving only a set of aerodynamic forces in the z direction acting on the nodes of the wing's upper surface. These forces may induce a resultant moment about either the X or Y axis of the wing, however; there are no aerodynamic moments applied at the individual nodes (i.e. $M_x = M_y = 0$). This results in the following set of 3N (N is the number of upper surface nodes) simultaneous equations:

$$\underset{3N\times N}{\begin{bmatrix} C_{zz} \\ C_{\theta_x z} \\ C_{\theta_y z} \end{bmatrix}} \underset{N\times 1}{\begin{Bmatrix} F_z \end{Bmatrix}} = \underset{3N\times 1}{\begin{Bmatrix} \hat{z} \\ \theta_x \\ \theta_y \end{Bmatrix}} \tag{8}$$

Note, however, that this set of equations can be separated into three independent sets of N simultaneous equations.

$$[C_{zz}]_{NxN} \quad \{F_z\}_{Nx1} = \{\dot{z}\}_{Nx1} \tag{9a}$$

$$[C_{\theta_x z}]_{NxN} \quad \{F_z\}_{Nx1} = \{\theta_x\}_{Nx1} \tag{9b}$$

$$[C_{\theta_y z}]_{NxN} \quad \{F_z\}_{Nx1} = \{\theta_y\}_{Nx1} \tag{9c}$$

Each of these can be solved independently from the others.

Equation 9c is of most importance to the divergence problem. As will be shown next, the aerodynamic forces are related to the local angle of attack of the wing. This local angle of attack can be related to the displacement θ_y either directly or indirectly, depending upon the manner in which the aerodynamic and structural models are combined. Consequently, Eq 9c is most suitable for developing into the eigenvalue problem.

Aerodynamic Model

The next step in developing the eigenvalue problem is to develop a workable aerodynamic model. The foundation for this model will be the tangential flow condition as developed by Ashley and Landahl (Ref 1). It relates the local angle of attack to the vortex distribution which in turn can be related to the lift distribution. However, this relation is difficult to work with and will be simplified. The simplification is accomplished with a doublet lattice modeling technique. This will leave the tangential flow condition in a form that can be combined with Eq 9c to form the eigenvalue problem. The doublet lattice method is described in more detail in Appendix A.

The wing is regarded as a thin wing. This allows it to be modeled as a sheet of pressure doublets. The strength of a pressure doublet corresponds to the strength of a horseshoe vortex as it is shrunk to a point. This includes the effects of the trailing portions of the vortex and allows the tangential flow relation to be formulated (Ref 1):

$$w(x,y,0) = \frac{1}{4\pi} \int\int_{S_{wing}} \frac{\gamma(x_1,y_1)}{(y-y_1)^2} \left[1 + \frac{(x-x_1)}{\sqrt{(x-x_1)^2 + (y-y_1)^2}} \right] dx_1 dy_1 \qquad (10)$$

where $\gamma(x_1,y_1)$ is the strength of the pressure doublet or vortex sheet at the point (x_1,y_1). This equation relates the component of the fluid velocity in the z direction at the wing's surface to the pressure doublet distribution. For wings at small angles of attack, the w component of the fluid velocity can be approximated by:

$$w(x,y,0) = U_\infty \frac{\partial z_a}{\partial x} = -U_\infty \alpha(x,y) \tag{11}$$

This allows the local angle of attack of a point $(x_i,y_i,0)$ to be written in terms of the doublet distribution:

$$\alpha(x_i,y_i) = \frac{-1}{4\pi U_\infty} \iint_{S_{wing}} \frac{\gamma(x_1,y_1)}{(y_i-y_1)^2} \left[1 + \frac{(x_i-x_1)}{\sqrt{(x_i-x_1)^2 + (y_i-y_1)^2}}\right] dx_1 y_1 \tag{12}$$

For the divergence problem, it is advantageous to obtain the vortex strength (Γ) as a function of the wing's geometry and flow conditions. The reason for this is that the vortex distribution is related to the normal lift distribution by: (Ref 4)

$$L = \int_0^c \rho_\infty U_\infty \gamma(x,y)\, dx \tag{13}$$

where L is the lift per unit span. This relates the lift to the wing's geometry. If discretized properly, the lift forces can be combined with the equilibrium equation to form the eigenvalue problem. However, the above tangential flow integral equation is very difficult to invert using analytical methods. If the wing is modeled with the doublet lattice method, the integral equation is transformed to a matrix equation. The vortex or doublet distribution can then be found by simply inverting a matrix of aerodynamic coefficients.

The wing is divided into a finite number of aerodynamic panels (see Fig 2). Each panel contains a control point (x_i,y_i), at which

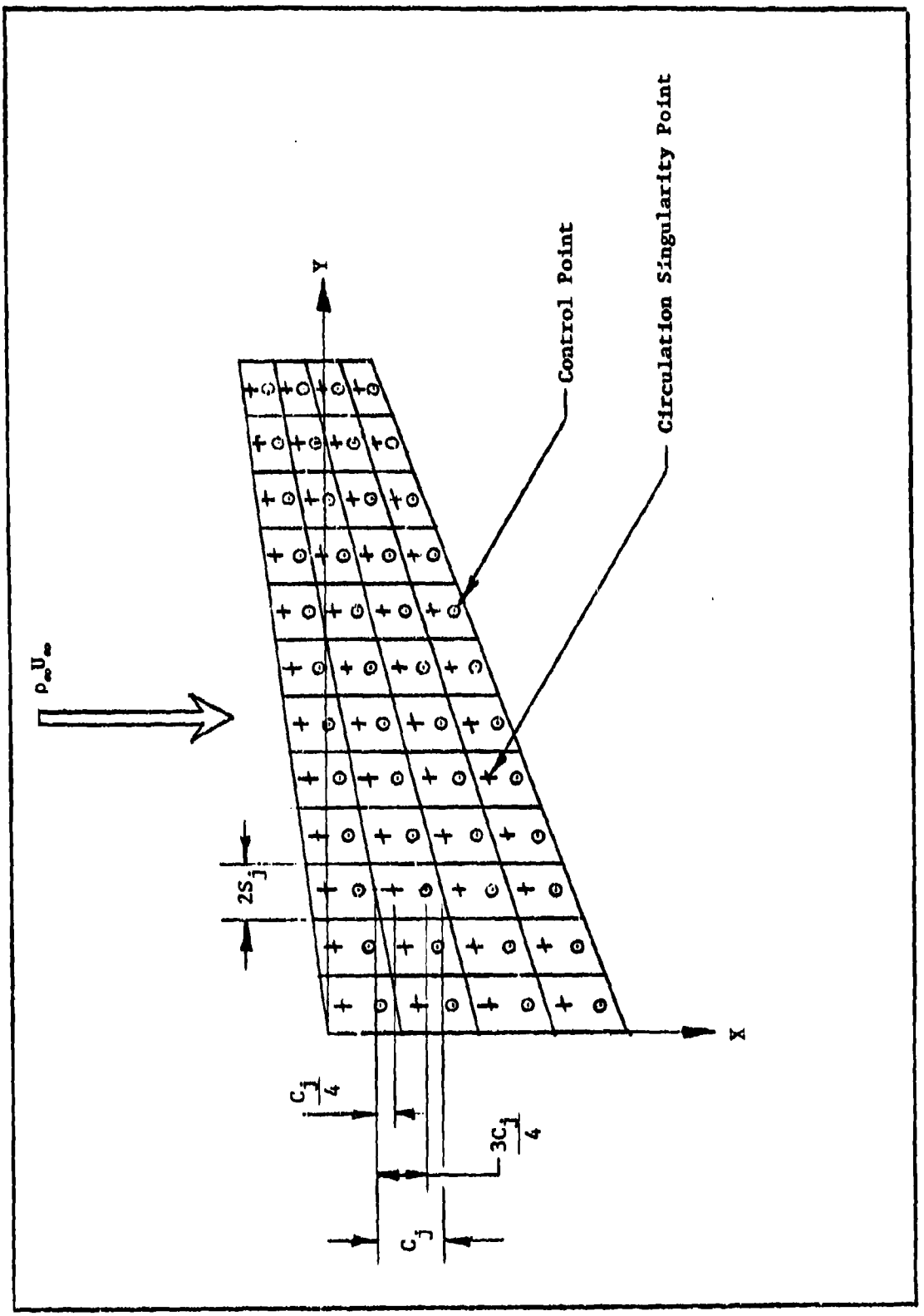

Figure 2. Doublet Lattice Aerodynamic Model

the angle of attack is known, and a point (x_j,y_j) for locating a vortex singularity. For an individual panel the vorticity (circulation per unit area) is approximated by a circulation per unit span acting along a constant cord line through the point (x_j,y_j). This is achieved by representing $\gamma(x_1,y_1)$ with a Dirac delta function

$$\gamma(x_1,y_1) = \Gamma(y_1)\ \delta(x_1 - x_j) \tag{14}$$

Substituting this into equation 12 and noting that

$$\int_A^B f(t)\ \delta(t - t_o)\ dt = f(t_o) \qquad \text{for } A < t_o < B \tag{15}$$

allows the integration over x_1 to be performed:

$$U_\infty\ \alpha(x_1,y_i) = -\frac{1}{4\pi} \sum_{j=1}^{N} \int_{y_j-S_j}^{y_j+S_j} \frac{\Gamma(y_1)}{(y_i-y_1)^2} \left[1 + \frac{(x_i-x_j)}{\sqrt{(x_i-x_j)^2+(y_i-y_1)^2}}\right] dy_1$$

$$N = \text{number of panels} \tag{16}$$

The circulation $\Gamma(y_1)$ can be brought outside the integral if it is assumed to be constant across the span of each panel. The remaining integral is an improper integral of the second kind. For a number of the panels there are singularity points at $y_1 = y_i$. However, it can be integrated using Mangler's principal-value technique (Ref 1).

$$U_\infty \alpha(x_i,y_i) = \frac{-1}{4\pi} \sum_{j=1}^{N} \Gamma_j \int_{y_j-S_j}^{y_j+S_j} \frac{1}{(y_i-y_1)^2} \left[1 + \frac{(x_i-x_j)}{\sqrt{(x_i-x_j)^2+(y_i-y_1)^2}} \right] dy_1$$

$$= \sum_{j=1}^{N} \left[\frac{-1}{4\pi(x_i-x_j)} \left\{ \frac{(x_i-x_j) + \sqrt{(x_i-x_j)^2 + (y_i-y_j-S_j)^2}}{y_i - y_j - S_j} \right.\right.$$

$$\left.\left. - \frac{(x_i-x_j) + \sqrt{(x_i-x_j)^2 + (y_i-y_j+S_j)^2}}{y_i - y_j + S_j} \right\} \right] \Gamma_j \qquad (17)$$

This equation can now be written in matrix form:

$$U_\infty \{\alpha_i\} = [A_{i,j}] \{\Gamma_j\} \qquad (18)$$

where

U_∞ = free stream velocity

$\{\alpha_i\}$ = the angles of attack of the set of control points (x_i,y_i), i=1, . . . N

$[A_{i,j}]$ = matrix of aerodynamic influence coefficients

$$A_{i,j} = \frac{-1}{4\pi\bar{x}} \left\{ \frac{\bar{x} + \sqrt{\bar{x}^2 + (\bar{y} - S_j)^2}}{\bar{y} - S_j} \right.$$

$$\left. - \frac{\bar{x} + \sqrt{\bar{x}^2 + (\bar{y} + S_j)^2}}{\bar{y} + S_j} \right\}$$

$$\bar{y} = y_i - y_j$$

$$\bar{x} = x_i - x_j$$

$\{\Gamma_j\}$ = the strengths of circulation singularities located at the points (x_j, y_j) j=1, . . . N

The circulation distribution is obtained by simply multiplying the equation by the inverse of the aerodynamic matrix:

$$\{\Gamma_j\} = U_\infty \left[A_{i,j} \right]^{-1} \{\alpha_i\} \tag{19}$$

For an individual panel, the lift per unit span is related to the circulation by:

$$L_j = \rho_\infty U_\infty \Gamma_j \tag{20}$$

or in matrix form:

$$\{L_j\} = \rho_\infty U_\infty \{\Gamma_j\} = \rho_\infty U_\infty^2 \left[A_{i,j} \right]^{-1} \{\alpha_i\} \tag{21}$$

The total lift of each panel is found by multiplying L_j by the span length of the panel.

$$\{L_j\} = \rho_\infty U_\infty \left[2S_j \right] \{\Gamma_j\} = \rho_\infty U_\infty^2 \left[2S_j \right] \left[A_{i,j} \right]^{-1} \{\alpha_i\} \tag{22a}$$

If the span length is the same for all panels:

$$\{L_j\} = 2\rho_\infty U_\infty S \{\Gamma_j\} = 2\rho_\infty U_\infty^2 S \left[A_{i,j} \right]^{-1} \{\alpha_i\} \tag{22b}$$

This effectively replaces the continuous pressure distribution with a set of forces acting at the singularity point locations. Each force depends upon the angle of attack at the control points of the other

panels, which may vary from panel to panel. After the angles of attack of the aerodynamic panels are related to the rotational degrees of freedom at the structural nodes, the aerodynamic and structural models can be combined to form the eigenvalue problem.

Combination of Aerodynamic and Structural Models

The final obstacle in formulating the eigenvalue problem is encountered when combining the aerodynamic and structural models. The local angle of attack at the aerodynamic panel control points must be related to the rotational degrees of freedom at the structural nodes. It may be helpful to consider a rectangular wing which has a simple flat plate for its load bearing structure. The structure is modeled by a set of nodes connected by quadrilateral plate elements (see Fig 3). An aerodynamic planform can be overlaid upon the structural model such that the aerodynamic singularity points coincide with the structural nodes. This allows the aerodynamic forces to be applied directly to the nodes.

There are several ways in which the local angle of attack of the control points can be related to the rotational degrees of freedom. One method is to assume that each aerodynamic panel acts as a flat plate. This allows the angle of attack at a control point to be approximated by the angle of attack at the singularity point of the same panel. Since the singularity point coincides with the node, the angle of attack at the singularity point is the rotation at the node. Thus, the aerodynamic and structural models could be combined directly to form the eigenvalue problem. However, this method may incur

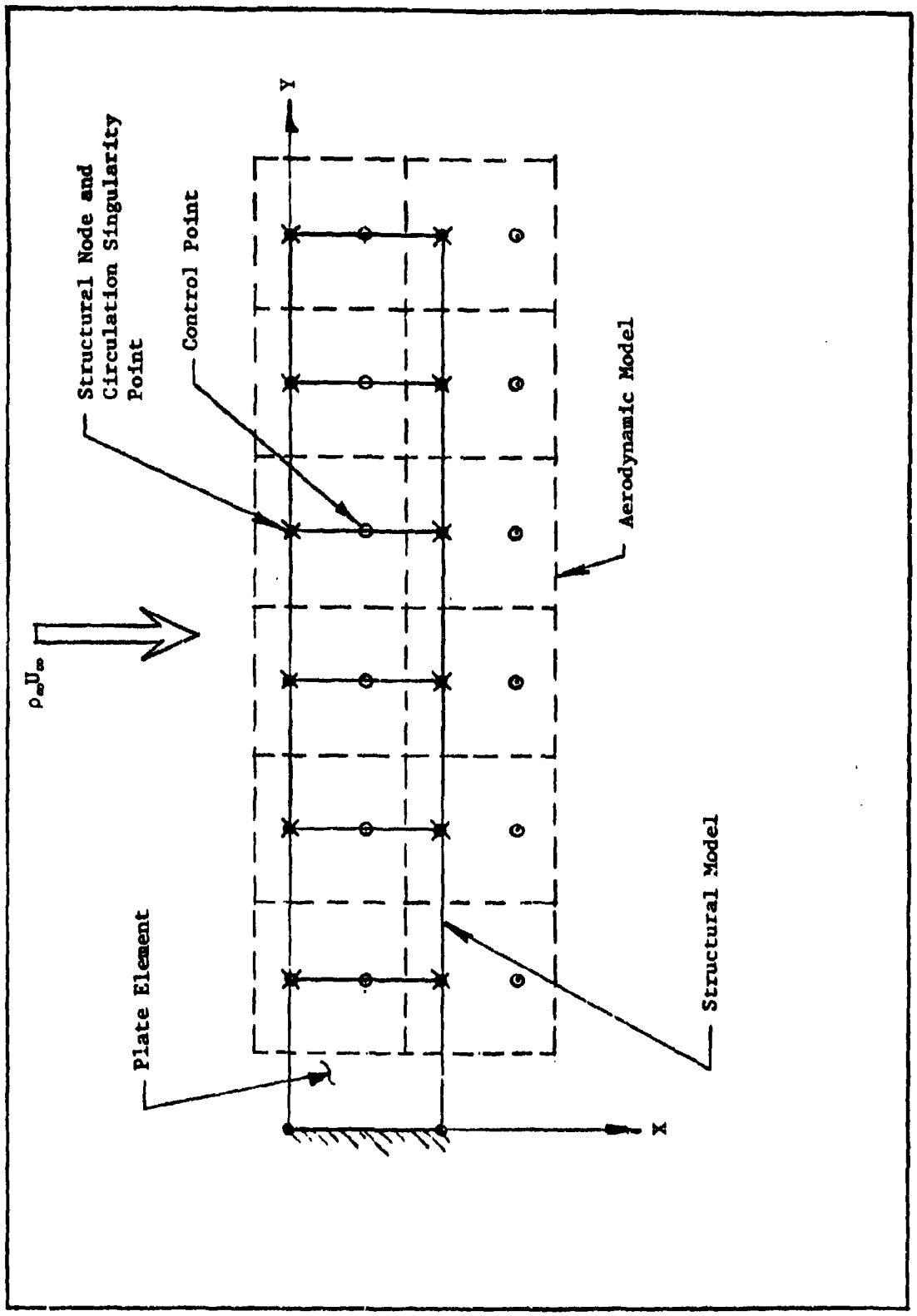

Figure 3. Example Flat Plate Wing

problems because it allows discontinuities across the aerodynamic panel borders.

A second method assumes that the aerodynamic planform is rigid in the X direction. The angle of attack for a given span station is found by dividing the difference between the displacements of the leading edge and trailing edge structural nodes by the structural chord length. This angle is used for the angle of attack of all control points along the chord of that particular span-wise station. In this manner the aerodynamic model is indirectly combined with the structural model to form the eigenvalue problem.

Both of the above methods provide similar results. They use an effective angle to approximate both the local angle of attack at the aerodynamic control points and the rotational degrees of freedom at the structural nodes. The final form of the eigenvalue problem is formulated by substituting the lift forces of Eq 22b into the equilibrium Eq 9c, and replacing both the local angle of attack α and the rotational degrees of freedom θ_y with the effective angle θ_{eff}.

$$4\,(S)\left(\frac{\rho_\infty U_\infty^2}{2}\right)\left[\,C_{\theta z}\,\right]\left[\,A_{ij}\,\right]^{-1}\{\theta_{eff_i}\} = \{\theta_{eff_j}\} \qquad (23)$$

The lowest value of the eigenvalue ($1/2\ \rho_\infty U_\infty^2$) is the divergence dynamic pressure, from which the divergence speed can be readily determined. The flexibility and aerodynamic influence coefficients are easily determined with the help of a computer, making the eigenvalue problem particular suitable to computer aided eigenvalue analysis techniques.

A wing with an aluminum box structure (complex structures are discussed in the next section) was analyzed using both methods for obtaining the effective angle θ_{eff}. Figure 4 compares these results with the results obtained by using NASTRAN's capabilities to determine the divergence speed. (The NASTRAN computer program is discussed in more detail later.) As is evident from Fig 4, both methods for combining the aerodynamic and structural models produce nearly identical results. The variation of divergence speed with sweep angle also correlates with the results obtained from NASTRAN if the differences in the two methods and NASTRAN are accounted for (NASTRAN used a strip theory model and assumed a symmetric lift distribution, resulting in lower values), indicating the method to be valid. The second method for approximating an effective angle of attack will be used in the analysis of the test wing. It will provide an accurate approximation for the local angle of attack since the test wing has a simple box structure.

Effects of Complex Wing Structures

For a simple rectangular wing, such as the flat plate example (Fig 3), it is easy to visualize how the aerodynamic grid might be directly overlaid on to the structural nodes. However, sweeping the wing forward complicates the problem since it can be done in several ways.

One method is to "sweep" the wing forward in such a manner that the root and the tip remain parallel to the flow (Fig 5). This method allows the aerodynamic representation to remain simple but "skews" the structural elements so that the nodes remain aligned with the flow. A second method is to "rotate" the wing forward (Fig 6). This allows the structural representation to stay the same but "skews"

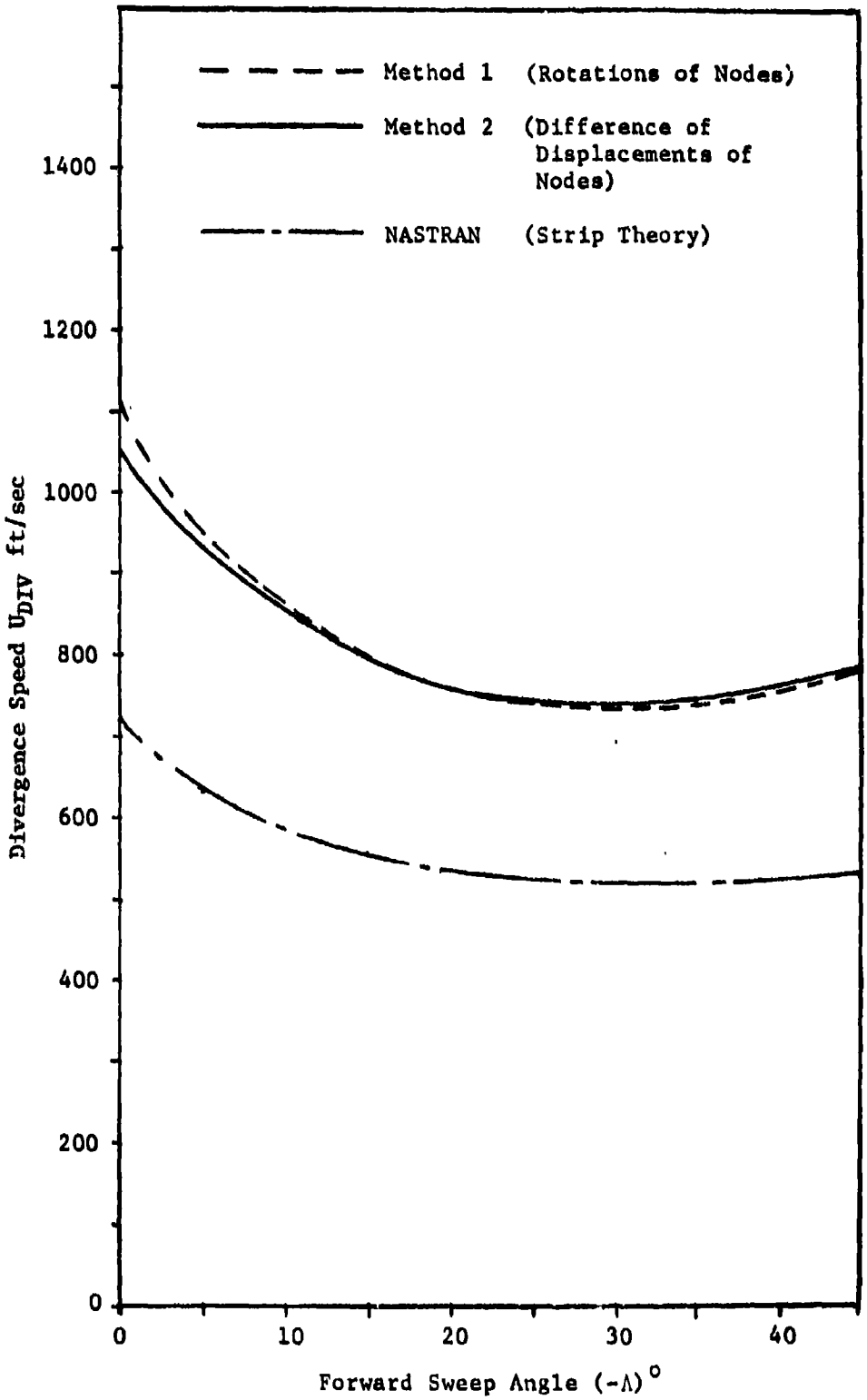

Figure 4. Comparison of Methods for Obtaining Divergence Speeds.

the aerodynamic boxes so that the aerodynamic grid points coincide with the structural nodes. With this method, the aerodynamic panels do not align in the chord-wise direction. This may or may not be troublesome, depending on the manner in which the effective angle of attack is found.

The flat plate wing of Fig 3 is not affected by the pitfalls of either method. It is represented by in-plane plate elements which do not have a strong dependence upon their shape to provide out-of-plane bending stiffness. Unfortunately, this simple wing model is not very prevalent among airplanes. A more common wing structure might be represented by the box structure shown in Fig 1. This structure is affected by the manner in which it is swept forward. Requiring the nodes to be aligned with the flow as the wing is swept forward, also aligns the chord-wise shear panels with the flow. This changes the stiffness characteristics of the structure as it is swept forward. As compared to the rotated wing, the swept wing will have a larger torsional stiffness and a smaller bending stiffness. However, for the simple box wing to be studied, this difference will be small. Thus, the first method, in which the wing is "swept" forward, will be used to analyze the test wing.

Remarks

The method described above for determining the divergence speed may appear to be contrived. The method might not be applicable to wings of arbitrary shape and the test wing might seem to be designed around this method. However, it should be pointed out that the purpose

of this study is to quantitatively determine how the divergence speed of a wing at a given sweep angle is affected by the orientation of the composite laminates making up the wing's structure. The material and structural properties of the forward swept, composite wing are represented by the flexibility matrix. The aerodynamic properties are represented by the aerodynamic matrix. Any variation in the structure or sweep angle is reflected in these two matrices, causing the divergence speed represented by the eigenvalue to vary accordingly.

This method can be applied to wings in either symmetric or antisymmetric flight. Symmetry is accounted for by adding the effects of the left wing to the aerodynamic matrix. The divergence speed for a wing in symmetric flight will then be less than that for the same wing with an antisymmetric lift distribution. However, this has no affect on the manner in which composite fiber orientation affects the divergence speed. Therefore, an antisymmetric lift distribution is assumed because it simplifies the formulation of the aerodynamic matrix.

III. Analysis of Example Wings

Introduction

The previous chapter developed an eigenvalue problem for finding the divergence speed of forward swept wings. A computer program for formulating and solving this eigenvalue problem was written and applied to a series of example wings. The computer program used NASTRAN to determine the flexibility matrix; calculated the aerodynamic matrix from Eq 18; solved the eigenvalue problem with an inverse power solution technique; and calculated the divergence speed from the lowest eigenvalue.

First, an aluminum wing was analyzed. Its divergence speed was calculated for different sweep angles to provide a basis of comparison with other methods. Then, the upper and lower surfaces of the wing were changed to composite laminates. For a given sweep angle the composite fiber orientations were varied. The divergence speeds were calculated for the various fiber orientations and compared. The results of this analysis are presented in Chapter 5. A more detailed description of this procedure follows.

Description of Example Wings

The wings to be analyzed have basically a cantilevered box structure, as is shown in Fig 7. They are composed of seven ribs and two spars each and are encased within a thin airfoil. The particular dimensions of both the aerodynamic planform and the structural box are shown in the figure. The wings are swept forward such that the total area of the wing remains constant. The lengths

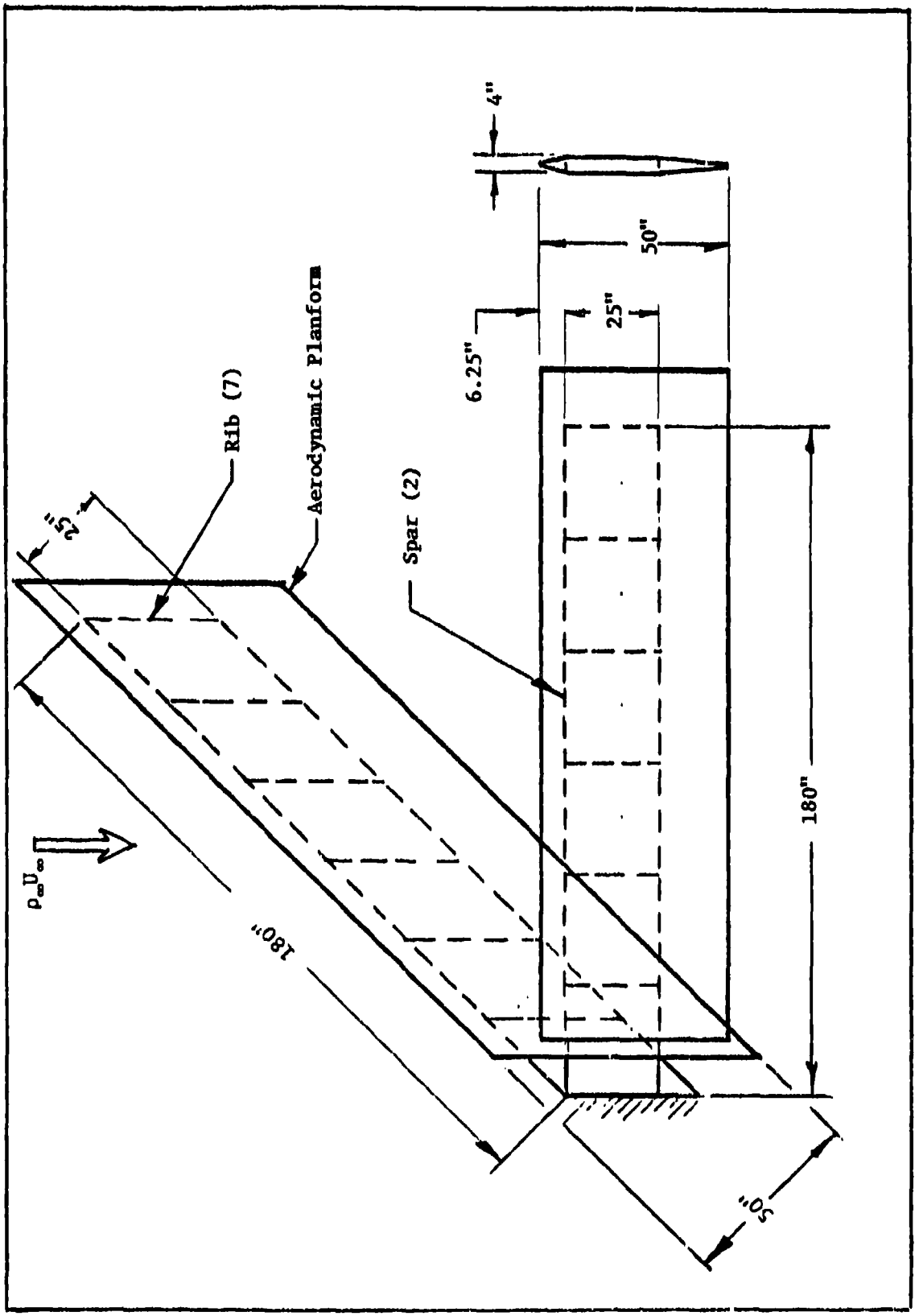

Figure 7. Example Wing Model

of the spars remain constant while the rib lengths are allowed to increase as the wings are swept forward. The ribs always remain parallel to the flow. This allows the basic structural box dimensions to remain constant as the wings are swept forward. It also permits the structure and aerodynamic planform of each wing to be modeled in a manner that provides for the easy combination of the two.

Structural Model

The wings defined above are each represented by 28 nodes, 14 on the upper surface and 14 directly below them on the lower surface. Each node is located at the junction of a rib, a spar, and the upper or lower surface. The four nodes at the root of each wing are totally fixed to cantilever the structure. The rib and spar members are represented by shear panels and rod elements. The rod elements are distributed so that each shear panel has rod elements on all four sides (some of the rod elements are shared between shear panels). These elements have aluminum material properties. The material properties and the cross sectional dimensions of these elements remain the same for every case considered.

The upper and lower surfaces are represented by thin plate elements. For the aluminum wings, there are 12 plate elements, 6 on the upper surface and 6 on the lower surface. Each element is .0525 in. thick. For the composite wings, there are 120 plate elements. Each aluminum plate element is replaced by 10 composite plate elements .00525 in. thick. Each element represents a composite

lamina and the 10 elements are connected to the same 4 nodes. This builds up a 10 layer composite laminate for representing the wing surface. The principal fiber directions of each of these layers can be oriented differently to vary the structural characteristics of the wing.

Two cases will be considered. These cases are defined in Fig 8 and Fig 9. For both cases, the principal fiber direction θ will be varied from 0° to 50° ahead of the structural sweep axis for several wing sweep angles. The computer program NASTRAN is used to calculate the flexibility matrix coefficients for each instance. The geometric and material properties of the structure and its elements are input to NASTRAN via the appropriate data cards to permit NASTRAN to formulate the elemental stiffness matrices and assemble them into the structural stiffness matrix.

The different methods for combining the structural and aerodynamic models require different flexibility matrices. For both methods, a unit load is applied to the i^{th} upper surface node, while all other forces are zero. This is done in turn to each of the upper surface nodes. For each load case NASTRAN solves the equilibrium equations:

$$\{F\} = [\,k\,]\,\{\delta\} \tag{4}$$

for all nodal displacements. Only the displacements for the upper surface nodes are output.

The direct combination method uses the rotations output by NASTRAN for the flexibility matrix. The rotations about the y-axis of the j^{th} upper surface nodes, caused by a unit load at the i^{th} node,

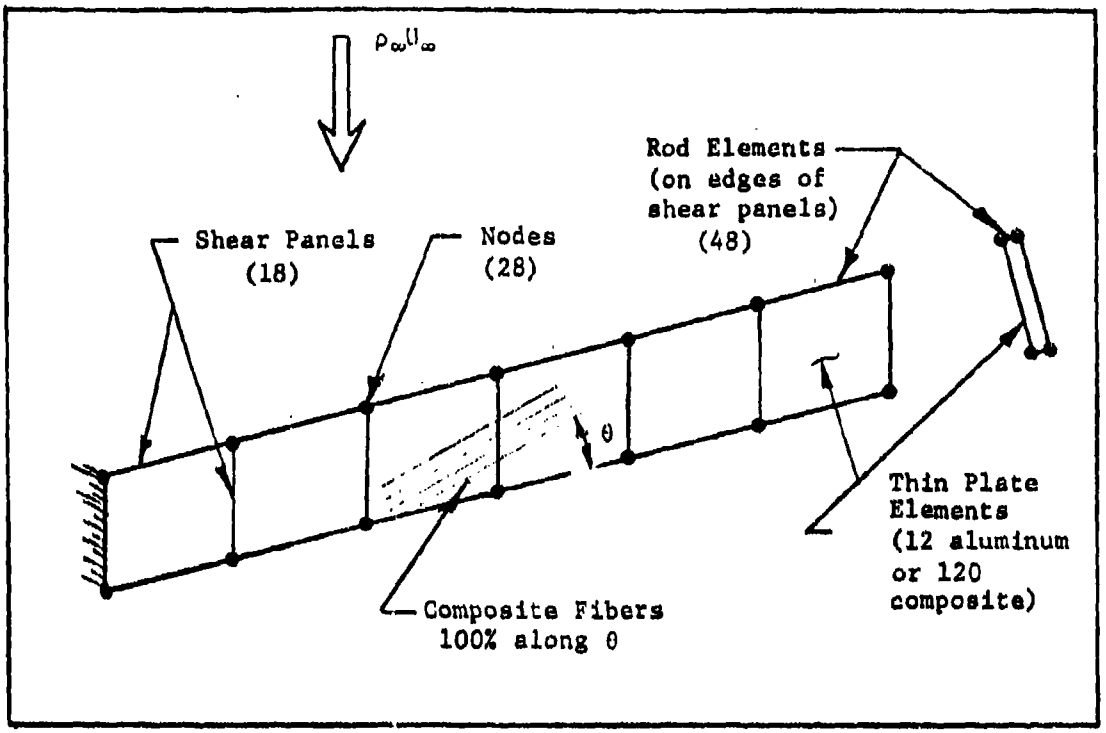

Figure 8. Case 1; 100% of Fibers Oriented Along the θ Direction

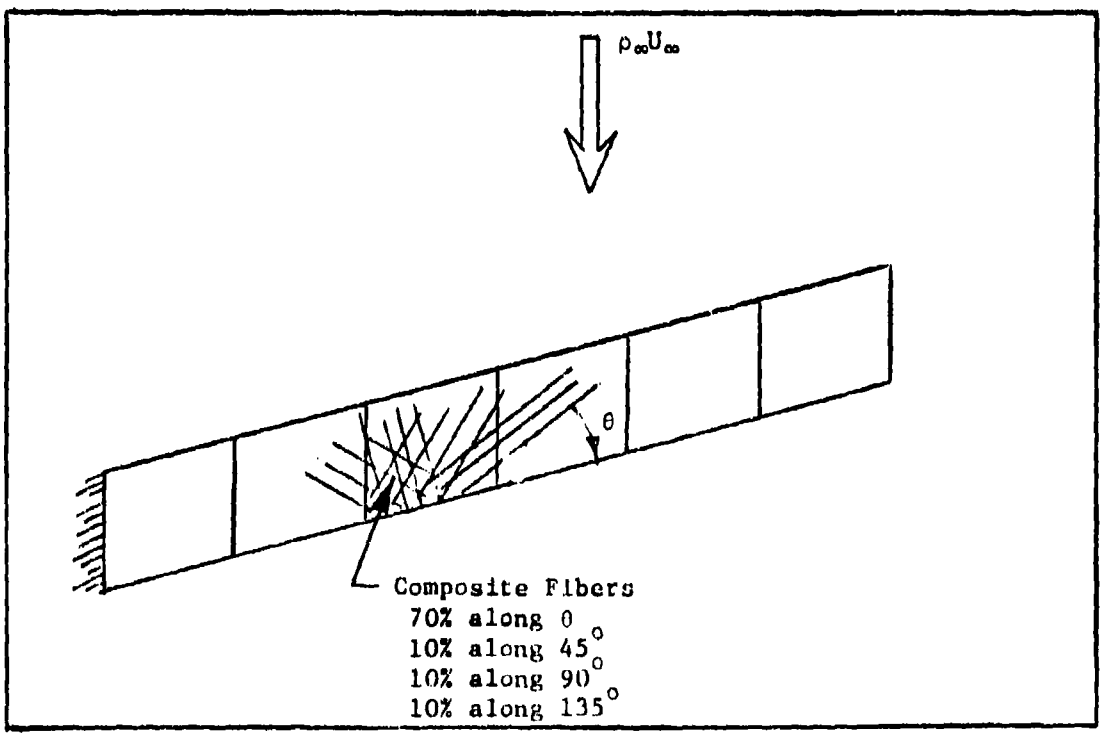

Figure 9. Case 2; 70% of Fibers Oriented Along the θ Direction

corresponds to the C_{ji} element of the flexibility matrix. Thus, NASTRAN directly computes an entire column of the flexibility matrix for each unit load force set.

The indirect combination method requires additional calculations. For a unit load at the i^{th} node, the difference in z displacements between the j and j + 1 nodes (The j and j + 1 nodes are, respectively, the leading and trailing edge nodes of a given span-wise station.) is divided by the structural distance between the j and j + 1 nodes. This calculated angle is then used for the C_{ji} and $C_{j+1,i}$ elements of the flexibility matrix.

The indirect method is used for the eigenvalue analysis of the various wings.

Aerodynamic Model

The aerodynamic planform is attached to the upper surface of the structure and is sectioned into symmetric panels as shown in Fig 10. The vortex singularities are located at the quarter-chord mid-span point of each panel. This allows them to coincide with the upper surface nodes. The control points are located at the three-quarter chord mid-span position of each panel. The computer program automatically calculates these points for a given sweep angle. It then uses these coordinates to calculate the aerodynamic matrix elements according to Eq 17 and 18. The flexibility matrix calculated by NASTRAN is input into the program and multiplied by the inverse of the aerodynamic matrix. This sets up the eigenvalue problem:

$$4S \left(\frac{\rho_\infty U_\infty^2}{2} \right) [\, CA \,] \{\theta\} = \{\theta\} \qquad (24)$$

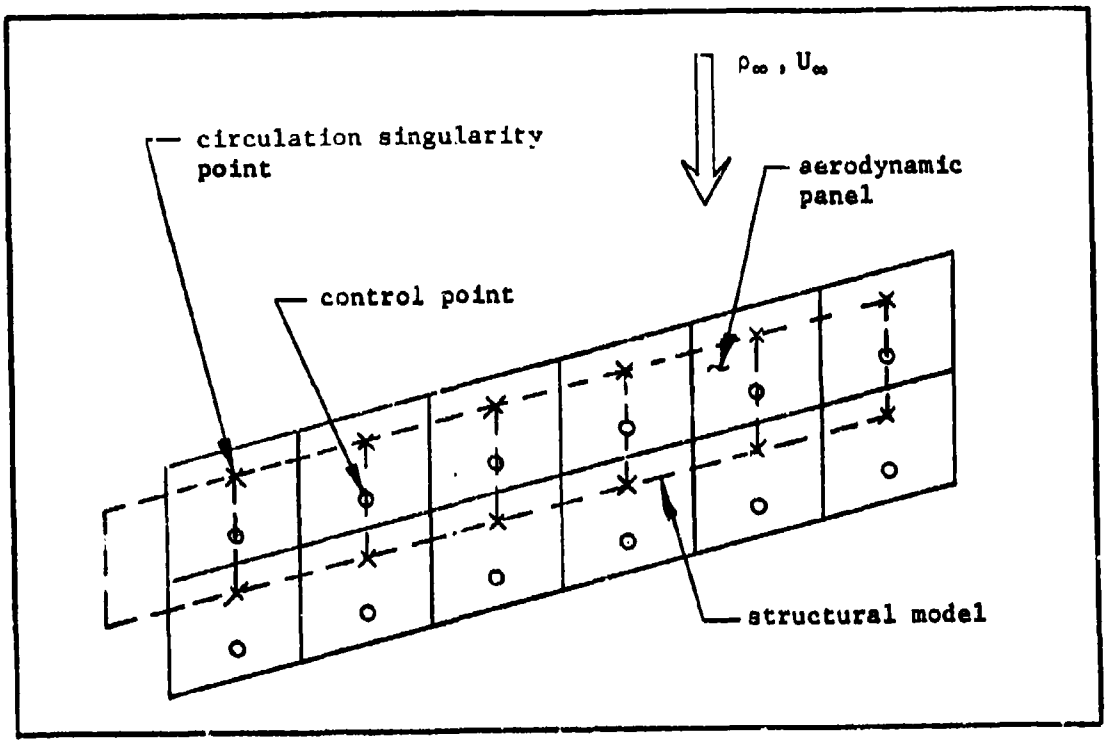

Figure 10. Example Wing Aerodynamic Model

Solution of the Eigenvalue Problem

An inverse power method is used to solve the eigenvalue problem. The method described by Hornbeck (Ref 3) was coded into FORTRAN and applied to the product matrix calculated above. This method is an iterative process that converges to the lowest eigenvalue.

The first step is to guess a solution for the eigenvector. This guess is then multiplied by the product matrix. The resultant vector is normalized to the value of the last element of its vector. This normalized vector is then multiplied by the produc matrix. The resultant vector is then normalized and again multiplied times the product matrix. This process continues until the normalized vectors

converge to the eigenvector. Similarly, the normalizing factor will converge to the inverse of the eigenvector ($\frac{1}{\lambda}$). This method always converges to the lowest eigenvalue, if it exists, usually in less than 6 iterations. From Eq 24 the eigenvalue is:

$$\lambda = 4S \left(\frac{\rho_\infty U_\infty^2}{2} \right) \tag{25}$$

The divergence speed is found by solving Eq 25 for U_∞

$$U_{DIV} = U_\infty = \left[\frac{\lambda}{2S\rho_\infty} \right]^{1/2} \tag{26}$$

A listing of both the NASTRAN data deck and the program written to calculate the aerodynamic matrix and solve the eigenvalue problem is included in appendix B. The results of this analysis are presented in the next chapter.

IV. Results

The wing defined in the previous chapter is used to study how the divergence speed varies with composite fiber orientation. First, divergence speeds of the aluminum wing at sweep angles of 0°, 15°, 25°, 35°, and 45° are calculated using the computer program described above. These values are plotted in Fig 4 and are used as a basis for comparison with other methods. For the two composite wing cases (Fig 8 and 9), the fiber orientation (θ) is varied in 5° increments from 0° to 50° ahead of the structural sweep angle. The divergence speed for each increment is computed and compared to the divergence speed for the composite wing with the fibers oriented at $\theta = 0$. This nondimensionalizes the divergence speed with the ratio $\frac{U_{DIV\ \theta}}{U_{DIV\ \theta=0}}$. Figures 11 and 12 plot this divergence speed ratio versus the composite orientation angle for the five sweep angles. Figure 11 considers the case where 100% of the composite fibers are oriented in the θ direction and Fig 12 considers the case where only 70% of the fibers are oriented in the θ direction (the remaining fibers are oriented at 90° and $\pm\ 45^{\circ}$ to the structural sweep angle). Figure 13 shows how U_{DIV} varies with sweep angle for $\theta = 0$.

From these results it is evident that the divergence problem of forward swept wings can be effectively controlled with laminated composites. As the principal fiber direction is swept ahead of the wing sweep angle, the divergence speed is seen to increase and reach a maximum. For wings of lesser sweep angles, the divergence problem is eliminated completely. This is true for both cases, although,

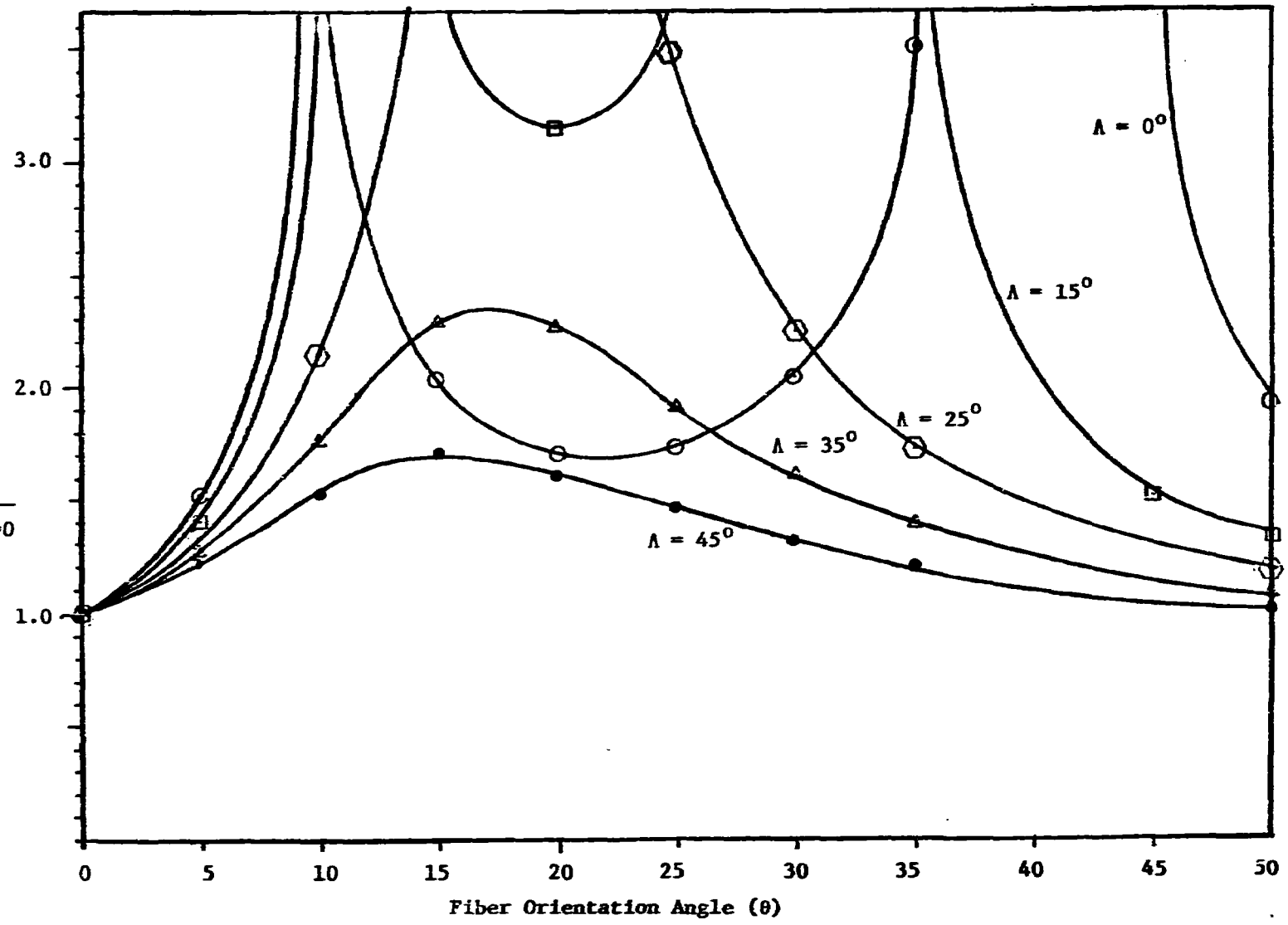

Figure 11. Comparison of Divergence Speeds for Case 1; 100% of Fibers Varied ($\Lambda = 0^{\circ}, 15^{\circ}, 25^{\circ}, 35^{\circ}, 45^{\circ}$)

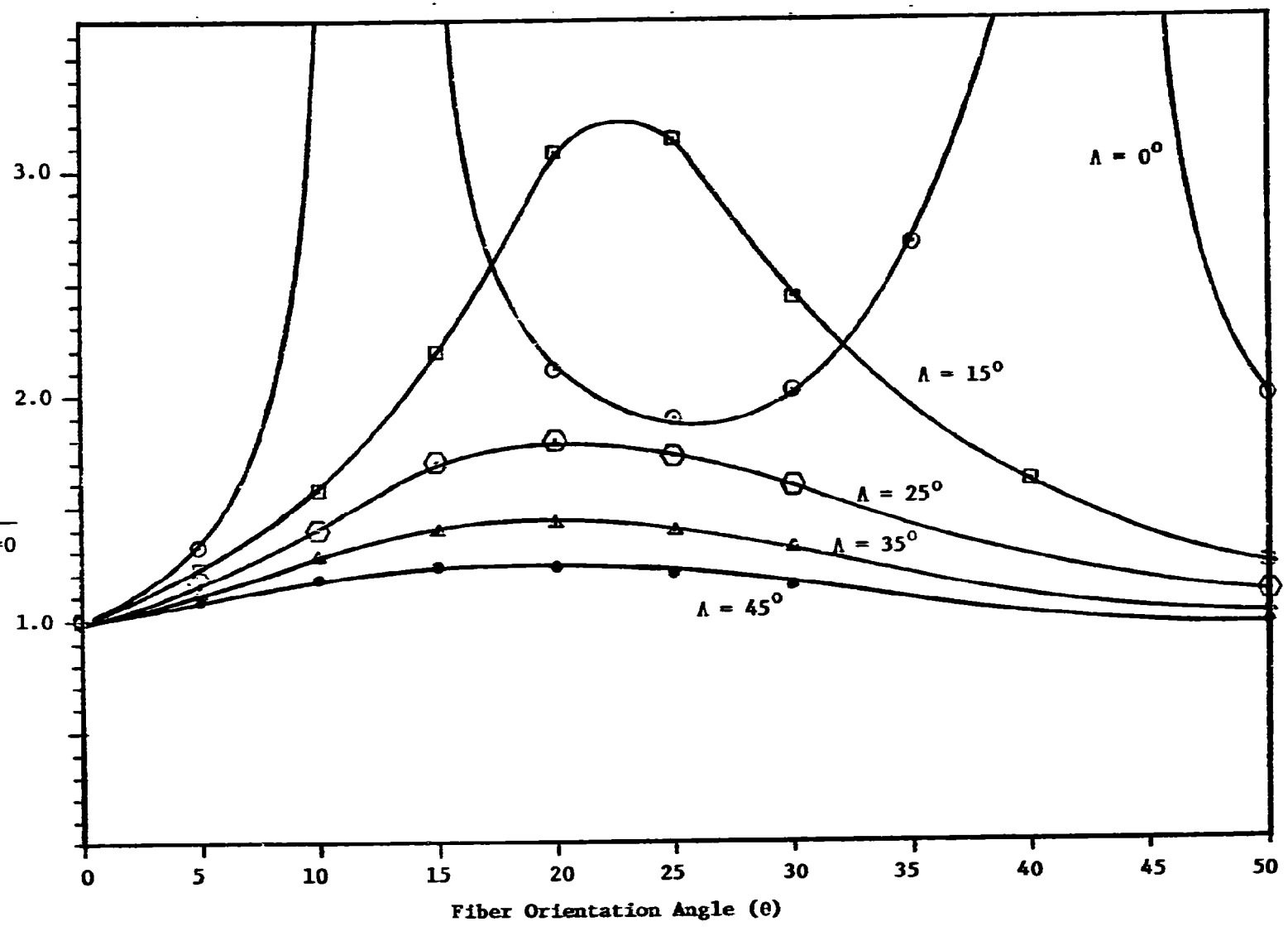

Figure 12. Comparison of Divergence Speeds for Case 2; 70% of Fibers Varied (Λ = 0°, 15°, 25°, 35°, 45°)

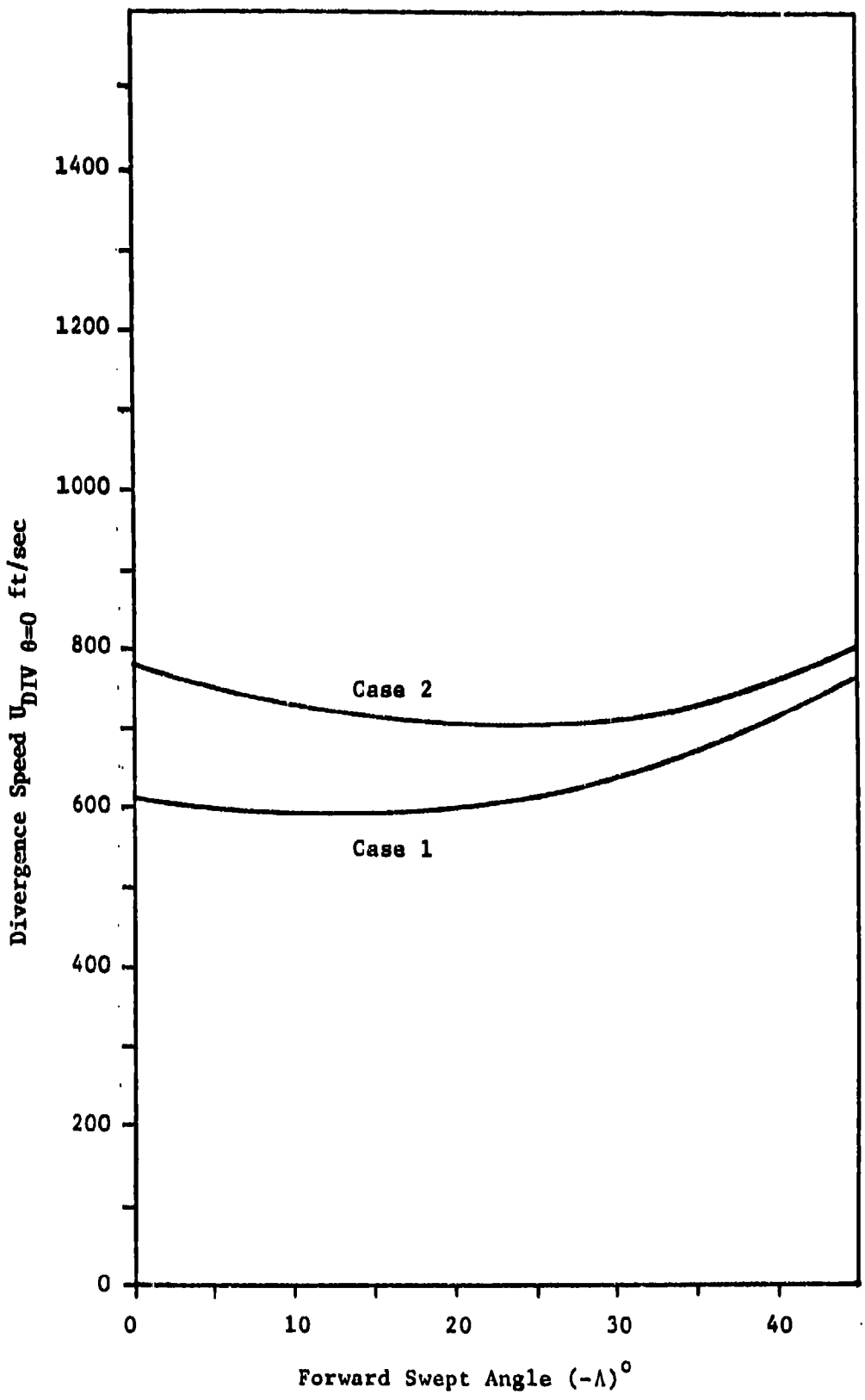

Figure 13. Variation of Divergence Speed with Sweep Angle for θ = 0

in varying degrees.

With the optimal choice of fiber orientation angle, the divergence speeds for case 1 (Fig 11) are increased by a factor of more than 1.5 for a 45° swept wing, and totally eliminated for wings swept 25° or less. Optimal fiber orientations are between 15° and 20° for wings swept more than 15°. The divergence speeds for case 2 (Fig 12) are not affected as drastically as they were for case 1, however; the same trends were obtained. Maximum values for case 2 for wings swept 15° or more occur for principal fiber orientations between 15° and 25°.

In both cases, the divergence speed varied unexpectedly for wings of small sweep angles. Unswept wings encountered two different maximums in the divergence speed variation at two different fiber orientations, around $\theta = 10^{\circ}$ and $\theta = 40^{\circ}$. No attempt has been made to explain this phenomenon other than to suggest that it might be caused by the coupling of the torsion and bending modes of divergence.

V. Conclusion

Summary

An eigenvalue problem was formulated to study the effects of composite material fiber orientations on the divergence speed of forward swept wings. This was accomplished by relating the aerodynamic forces to the wing deformations with the tangential flow condition. These deformations were related to structural properties by applying the static equilibrium equation. The aerodynamic and structural properties were modeled with a doublet lattice method and a finite element method, respectively. These modeling techniques simplify the appropriate force-displacement relations and allow the relations to be written in matrix form. The two force-displacement relations were combined to form the eigenvalue problem of Eq 23.

A computer program was written which used NASTRAN to calculate a flexibility matrix for the structure. It calculated the aerodynamic matrix from the doublet lattice method and solved the eigenvalue problem with an inverse power technique. The program was applied to two cases of swept wings. For the first case, 100% of the composite fibers were varied from 0° to 50° ahead of the structural sweep axis. For the second case, only 70% of the composite fibers were varied while the remaining fibers were held at 90° and $\pm 45^{\circ}$ to the structure-swept axis. Sweep angles from 0° to 45° were studied. The calculated divergence speeds for both cases are compared in Fig 11 and Fig 12.

Conclusions

Figures 11 and 12 indicate that the divergence problem of forward swept wings can be effectively controlled and possibly eliminated by using the proper composite fiber orientations. The divergence speed was found to increase and reach a maximum as the principal fiber direction was swept forward. The maximum values occurred for fibers oriented between 15° and 20° ahead of the structural sweep axis for wings swept forward 25° or more. This was found to be true for both cases, although, to a lesser extent for the case where only 70% of the fibers were varied.

The results obtained by this study concur with the results of both Krone (Ref 6) and Weisshaar (Ref 7) in affirming the feasibility of using laminated composites for controlling the divergence speed of forward swept wings. However, no attempt has been made to study the affects of composite materials on flutter, strength, fatigue or other problems of wing structures. Further study is required in these areas.

Bibliography

1. Ashley, H. and Landahl, M. Aerodynamics of Wings and Bodies. Reading, Massachusetts: Addison-Wesley Publishing Co., 1965.

2. Bisplinghoff, R., Ashley, H., and Halfman, R. Aeroelasticity. Reading, Massachusetts: Addison-Wesley Publishing Co., 1957.

3. Hornbeck, R. Numerical Methods. New York: Quantum Publishers, Inc., 1975.

4. Kuethe, A. M. and Schetzer, J. D. Foundations of Aerodynamics. New York: John Wiley & Sons, Inc., 1959.

5. MacNeal, R. H., Ed. The NASTRAN Theoretical Manual (Level 15). The University of Georgia, Athens: Computer Software Management and Information Center (COSMIC), NASA SP-221(01), 1972.

6. Przemieniecki, J. S. Theory of Matrix Structural Analysis. New York: McGraw Hill Book Co., 1968.

7. Holzbaur, S. "Swept-Forward Wings," Interavia, Vol 5, No. 7, pp. 380-382, 1950.

8. Krone, N. "Divergence Elimination with Advanced Composites," AIAA 1975 Aircraft Systems and Technology Meeting, No. 75-1009, August 1975.

9. Weisshaar, T. Aeroelastic Stability and Performance Characteristics of Aircraft with Advanced Composite Swept Forward Wing Structures. AFFDL-TR-78-116, Wright-Patterson AFB, Ohio; Air Force Flight Dynamics Laboratory, September 1978.

10. Eastep, F. Class Notes from MC 7.37: Unsteady Aerodynamics, School of Engineering, Air Force Institute of Technology, Winter Quarter, 1978.

Appendix A
Doublet Lattice Aerodynamic Model

The doublet lattice method incorporates the usual assumptions regarding thin airfoils and irrotationality to form a tangential flow equation. This equation relates the angle of attack of a given point on the wing surface to the strengths of the circulation vortices representing the wing. In most instances, the geometry of the wing is known and the problem is to determine the circulation distribution. This is most efficiently accomplished using matrix methods. The wing is discretized to allow the tangential flow equation to be written in matrix form. The equation can then be inverted and the circulation at a given point found in terms of the wing's geometry and the fluid velocity. From elementary aerodynamics, the circulation is related to the normal lift forces providing a useful method of determining the lift and drag forces and the resultant moments acting upon a wing.

The wing is regarded as a thin wing. This allows it to be modeled as a sheet of pressure doublets. The strength of a pressure doublet corresponds to the strength of a horseshoe vortex as it is shrunk to a point. This includes the effects of the trailing portions of the vortex and allows the tangential flow relation to be formulated (Ref 1):

$$w(x,y,0) = \frac{1}{4\pi}\iint \frac{\gamma(x_1,y_1)}{(y-y_1)^2}\left[1 + \frac{(x-x_1)}{\sqrt{(x-x_1)^2+(y-y_1)^2}}\right] dx_1 dy_1 \qquad \text{(A-1)}$$

where $\gamma(x_1,y_1)$ is the strength of the pressure doublet or vortex sheet at the point (x_1,y_1). This equation relates the component of

the fluid velocity in the z direction at the wing's surface to the pressure doublet distribution. For wings at small angles of attack, the w component of the fluid velocity can be approximated by:

$$w(x,y,0) = U_\infty \frac{\partial z}{\partial x} = -U_\infty \alpha(x,y) \qquad \text{(A-2)}$$

This allows the local angle of attack of a point $(x_i,y_i,0)$ to be written in terms of the circulation distribution:

$$\alpha(x_i,y_i) = \frac{-1}{4\pi U_\infty} \iint \frac{\gamma(x_1,y_1)}{(y_i-y_1)^2}\left[1 + \frac{(x_i-x_1)}{\sqrt{(x_i-x_1)^2+(y_i-y_1)^2}}\right] dx_1 dy_1 \qquad \text{(A-3)}$$

Howevar, in most instances, the vortex distribution is not known and it would be desirable to obtain the vortex strength at the point (x_1,y_1) in terms of the wing geometry. This is most effectively accomplished using matrix methods. Therefore, the next step is to discretize the wing to permit the tangential flow condition to be written in matrix form.

The wing is divided into a finite number of aerodynamic panels (see Fig 2). Each panel contains a control point (x_i,y_i), at which the angle of attack is known, and a point (x_j,y_j) for locating a vortex singularity. For an individual panel the vorticity (circulation per unit area) is approximated by a circulation per unit span acting along a constant chord line through the point (x_j,y_j). This is achieved by representing $\gamma(x_1,y_1)$ with a Dirac delta function:

$$\gamma(x_1,y_1) = \Gamma(y_1)\,\delta(x_i - x_j) \qquad \text{(A-4)}$$

Substituting this into Eq A-3 and noting that:

$$\int_A^B f(t)\ \delta(t-t_o)\ dt = f(t_o) \qquad \text{for } A < t_o < B \tag{A-5}$$

allows the integration over x_1 to be performed:

$$U_\infty\ a(x_i,y_i) = \frac{-1}{4\pi} \sum_{j=1}^{N} \oint_{y_j-S_j}^{y_j+S_j} \frac{\Gamma(y_1)}{(y_i-y_1)^2} \left[1 + \frac{(x_i-x_j)}{\sqrt{(x_i-x_j)^2+(y_i-y_1)^2}} \right] dy_1$$

N = number of panels (A-6)

The circulation $\Gamma(y_1)$ can be brought outside the integral if it is assumed to be constant across the span of each panel. The remaining integral is an improper integral of the second kind. For a number of the boxes, there are singularity points at $y_1 = y_i$. However, it can be integrated using Mangler's principal-value technique. (Ref 1)

$$U_\infty \alpha(x_i,y_i) = \frac{-1}{4\pi} \sum_{j=1}^{N} \Gamma_j \int_{y_j-S_j}^{y_j+S_j} \frac{1}{(y_i-y_1)^2} \left[1 + \frac{(x_i-x_j)}{\sqrt{(x_i-x_j)^2+(y_i-y_1)^2}} \right] dy_1$$

$$= \sum_{j=1}^{N} \left[\frac{-1}{4\pi(x_i-x_j)} \left\{ \frac{(x_i-x_j) + \sqrt{(x_i-x_j)^2 + (y_i-y_j-S_j)^2}}{y_i - y_j - S_j} \right.\right.$$

$$\left.\left. - \frac{(x_i-x_j) + \sqrt{(x_i-x_j)^2 + (y_i-y_j+S_j)^2}}{y_i - y_j + S_j} \right\} \right] \Gamma_j \qquad \text{(A-7)}$$

This equation can now be written in matrix form:

$$U_\infty \{\alpha_i\} = [A_{i,j}] \{\Gamma_j\} \qquad \text{(A-8)}$$

where

U_∞ = free stream velocity

$\{\alpha_i\}$ = the angles of attack of the set of control points (x_i, y_i), i=1, . . . N

$[A_{i,j}]$ = matrix of aerodynamic influence coefficients

$$A_{i,j} = \frac{-1}{4\pi\bar{x}} \left\{ \frac{\bar{x} + \sqrt{\bar{x}^2 + (\bar{y} - S_j)^2}}{\bar{y} - S_j} \right.$$

$$\left. - \frac{\bar{x} + \sqrt{\bar{x}^2 + (\bar{y} + S_j)^2}}{\bar{y} + S_j} \right\}$$

$$\bar{y} = y_i - y_j$$

$$\bar{x} = x_i - x_j$$

$\{\Gamma_j\}$ = the strengths of circulation singularities located at the points (x_j, y_j) j=1, . . . N

The circulation distribution is obtained by simply multiplying Eq A-8 by the inverse of the aerodynamic matrix:

$$\{\Gamma_j\} = U_\infty \left[A_{i,j} \right]^{-1} \{\alpha_i\} \tag{A-9}$$

For an individual panel, the lift per unit span is related to the circulation by:

$$L_j = \rho_\infty U_\infty \Gamma_j \tag{A-10}$$

or in matrix form:

$$\{L_j\} = \rho_\infty U_\infty \{\Gamma_j\} = \rho_\infty U_\infty^2 \left[A_{i,j} \right]^{-1} \{\alpha_i\} \tag{A-11}$$

This provides the lift per unit span for the individual aerodynamic panels. The total lift on each panel is found by multiplying L_j by the span length of each panel:

$$\{L_j\} = \rho_\infty U_\infty \{2S_j \Gamma_j\} \tag{A-12}$$

Summing the lift contributed by each panel gives the total lift for the wing.

$$L = \sum_{j=1}^{N} L_j = 2\rho_\infty U_\infty \sum_{j=1}^{N} S_j \Gamma_j \tag{A-13}$$

The drag forces (D_j from Fig 14) are:

$$D_j = L_j \sin \alpha \approx L_j \alpha \tag{A-14}$$

or

$$\{D_j\} = \{L_j \alpha_j\} = \rho_\infty U_\infty \{2S_j \Gamma_j \alpha_j\} \qquad \text{(A-15)}$$

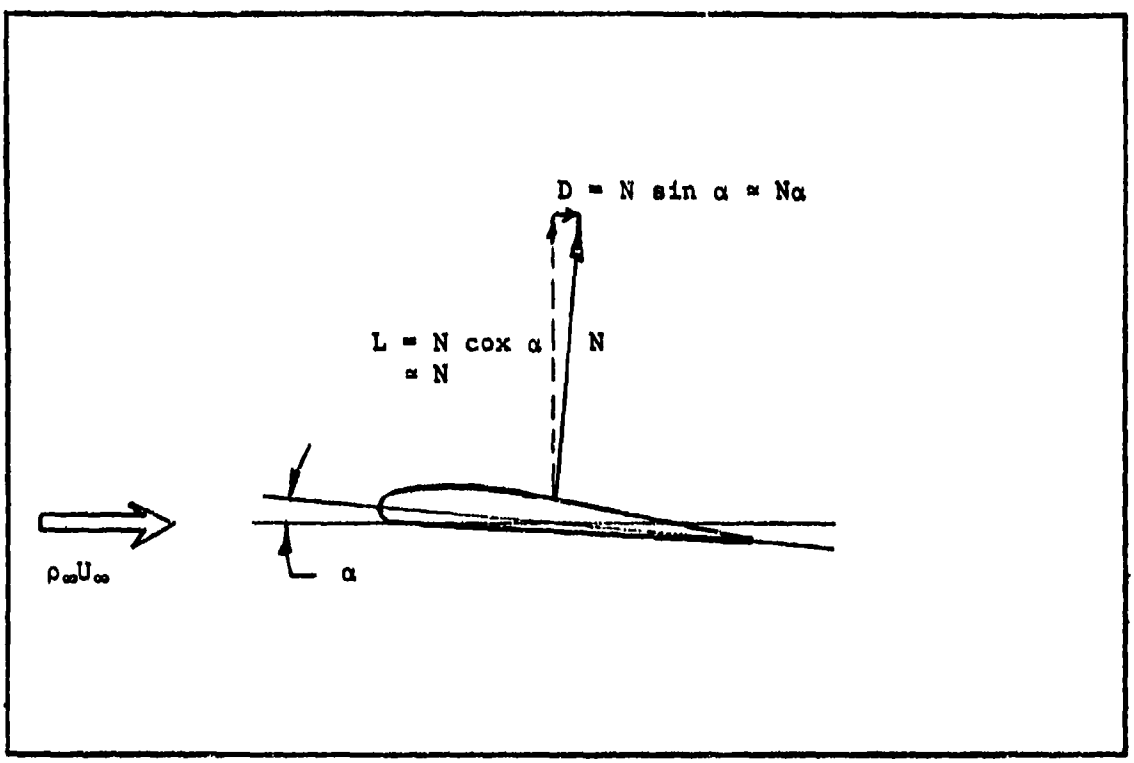

Figure 14. Definition of Wing Forces

Resultant moments about a given axis can be calculated from:

$$M_{x_o} = \sum_{j=1}^{N} L_j (x_j - x_o) \qquad \text{(A-16)}$$

$$M_{y_o} = \sum_{j=1}^{N} L_j (x_j - x_o) \qquad \text{(A-17)}$$

This method produces approximations to the actual aerodynamic forces. The accuracy of the method increases as the number of aerodynamic panels is increased. So far, the circulation singularity and control points, (x_j,y_j) and (x_i,y_i), have been arbitrarily located within the panels. Dispersing these points more evenly over the wing also increases the accuracy of the method. Locating the circulation singularities at the quarter-chord mid-span points, and the control points at the three quarter-chord mid-span points of each panel has been found to have the best results.

The doublet lattice method is applicable to wings of arbitrary trapezoidal shape. The aerodynamic panels need not be rectangular, allowing the method to be applied to tapered and swept wings. However, care should be used in selecting the panel size and the locations of the circulation singularities and control points for swept wings. The aerodynamic influence coefficients contain a possible singularity if the x-coordinate of a control point aligns with the x-coordinate of a circulation singularity from a different panel. This problem can be omitted by varying the span of each box with respect to its chord length. Changing either the number of span-wise panels or the number of chord-wise panels will usually solve the problem.

It is also possible to vary the size of a panel with respect to other panels. This allows the panels to be concentrated close to wing tips and edges where the circulation may change drastically. Likewise, panels can be dispersed over the central portions of the wing where little variation is expected.

The doublet lattice method can be applied to wings in symmetric

flight as well as antisymmetric flight. Symmetry can be accounted for by adding the effects of the left wing to the aerodynamic matrix. This is done by summing the effects of the corresponding aerodynamic panels of both the right and left wings on an element of the aerodynamic matrix, rather than the effects of only the panel on the right wing.

The doublet lattice method is easily handled with a computer and also lends itself to other purposes, such as the eigenvalue analysis developed in the body of this thesis.

Appendix B
Listing of Computer Programs

This appendix has two parts. The first part is a listing of the NASTRAN program used to calculate the flexibility coefficients. The geometric and structural data listed in the BULK DATA section are for an unswept wing with 100% of the fibers oriented along the sweep angle ($\theta = 0$). Varying the sweep angle affects only the grid point coordinates and varying the fiber orientation affects only the last column of the CQUAD2 element cards.

The second part of this appendix is a listing of the Aerodynamic and Eigenvalue Analysis program. It too, is for an unswept wing. The wing can be "swept" forward by changing the sweep angle on the DATA card. The wing can be "rotated" forward by also changing the locations of the circulation and control points appropriately.

N A S T R A N E X E C U T I V E C O N T R O L D E C K E C H O

```
ID CRY39,AFIT
TIME 5
APP DISP
SOL 1,0
CEND
```

CASE CONTROL DECK ECHO

```
CARD
COUNT
  1     TITLE=FLEXIBILITY MATRIX CALCULATION FOR A 30X WING
  2     SPC=1
  3     SET 1=5,7,9,11,13,15,17,19,21,23,25,27
  4     DISPLACEMENT(PRINT,PUNCH)=1
  5     SUBCASE 1
  6         LOAD = 5
  7     SUBCASE 2
  8         LOAD = 7
  9     SUBCASE 3
 10         LOAD = 9
 11     SUBCASE 4
 12         LOAD = 11
 13     SUBCASE 5
 14         LOAD = 13
 15     SUBCASE 6
 16         LOAD = 15
 17     SUBCASE 7
 18         LOAD = 17
 19     SUBCASE 8
 20         LOAD = 19
 21     SUBCASE 9
 22         LOAD = 21
 23     SUBCASE 10
 24         LOAD = 23
 25     SUBCASE 11
 26         LOAD = 25
 27     SUBCASE 12
 28         LOAD = 27
 29     BEGIN BULK
```

SORTED BULK DATA ECHO

CARD COUNT	1	2	3	4	5	6	7	8	9
1-	CQUAD2	601	5	3	7	5	1	0.000	
2-	CQUAD2	602	5	3	7	5	1	0.000	
3-	CQUAD2	603	5	3	7	5	1	0.000	
4-	CQUAD2	604	5	3	7	5	1	0.000	
5-	CQUAD2	605	5	3	7	5	1	0.000	
6-	CQUAD2	606	5	3	7	5	1	0.000	
7-	CQUAD2	607	5	3	7	5	1	0.000	
8-	CQUAD2	608	5	3	7	5	1	0.000	
9-	CQUAD2	609	5	3	7	5	1	0.000	
10-	CQUAD2	610	5	3	7	5	1	0.000	
11-	CQUAD2	611	5	4	5	6	2	0.000	
12-	CQUAD2	612	5	4	5	5	2	0.000	
13-	CQUAD2	613	5	4	5	5	2	0.000	
14-	CQUAD2	614	5	4	5	5	2	0.000	
15-	CQUAD2	615	5	4	5	5	2	0.000	
16-	CQUAD2	616	5	4	5	5	2	0.000	
17-	CQUAD2	617	5	4	5	5	2	0.000	
18-	CQUAD2	618	5	4	5	5	2	0.000	
19-	CQUAD2	619	5	4	5	5	2	0.000	
20-	CQUAD2	620	5	4	5	5	2	0.000	
21-	CQUAD2	621	5	7	11	9	5	0.000	
22-	CQUAD2	622	5	7	11	9	5	0.000	
23-	CQUAD2	623	5	7	11	9	5	0.000	
24-	CQUAD2	624	5	7	11	9	5	0.000	
25-	CQUAD2	625	5	7	11	9	5	0.000	
26-	CQUAD2	626	5	7	11	9	5	0.000	
27-	CQUAD2	627	5	7	11	9	5	0.000	
28-	CQUAD2	628	5	7	11	9	5	0.000	
29-	CQUAD2	629	5	7	11	9	5	0.000	
30-	CQUAD2	630	5	7	11	9	5	0.000	
31-	CQUAD2	631	5	8	12	10	6	0.000	
32-	CQUAD2	632	5	8	12	10	6	0.000	
33-	CQUAD2	633	5	8	12	10	6	0.000	

CAPT COUNT	1	2	3	4	5	6	7	8	9
34-	COUAD2	634	5	8	12	10	6	0.000	
35-	COUAD2	635	5	8	12	10	6	0.000	
36-	COUAD2	636	5	8	12	10	6	0.000	
37-	COUAD2	637	6	8	12	10	5	0.000	
38-	COUAD2	638	5	5	12	10	6	0.000	
39-	COUAD2	639	5	8	12	10	6	0.000	
40-	COUAD2	640	5	8	12	10	6	0.000	
41-	COUAD2	641	5	11	15	13	9	0.000	
42-	COUAD2	642	5	11	15	13	9	0.000	
43-	COUAD2	643	5	11	15	13	9	0.000	
44-	COUAD2	644	5	11	15	13	9	0.000	
45-	COUAD2	645	5	11	15	13	9	0.000	
46-	COUAD2	646	5	11	15	13	9	0.000	
47-	COUAD2	647	5	11	15	13	9	0.000	
48-	COUAD2	648	5	11	15	13	9	0.000	
49-	COUAD2	649	5	11	15	13	9	0.000	
50-	COUAD2	650	5	11	15	13	9	0.000	
51-	COUAD2	651	5	12	16	14	10	0.000	
52-	COUAD2	652	5	12	16	14	10	0.000	
53-	COUAD2	653	6	12	16	14	10	0.000	
54-	COUAD2	654	5	12	16	14	10	0.000	
55-	COUAD2	655	5	12	16	14	10	0.000	
56-	COUAD2	656	5	12	16	14	10	0.000	
57-	COUAD2	657	5	12	16	14	10	0.000	
58-	COUAD2	658	5	12	16	14	10	0.000	
59-	COUAD2	659	5	12	16	14	10	0.000	
60-	COUAD2	660	5	12	16	14	10	0.000	
61-	COUAD2	661	5	15	19	17	13	0.000	
62-	COUAD2	662	5	15	19	17	13	0.000	
63-	COUAD2	663	5	15	19	17	13	0.000	
64-	COUAD2	664	5	15	19	17	13	0.000	
65-	COUAD2	665	5	15	19	17	13	0.000	
66-	COUAD2	666	5	15	19	17	13	0.000	

CARD COUNT	1	2	3	4	5	6	7	8	9	10
57-	COUAD2	667	5	15	19	17	13	0.000		
58-	COUAD2	668	5	15	19	17	13	0.000		
59-	COUAD2	669	5	15	19	17	13	0.000		
70-	COUAD2	670	5	15	19	17	13	0.000		
71-	COUAD2	671	5	16	20	18	14	0.000		
72-	COUAD2	672	5	16	20	18	14	0.000		
73-	COUAD2	673	5	16	20	18	14	0.000		
74-	COUAD2	674	5	16	20	18	14	0.000		
75-	COUAD2	675	5	16	20	18	14	0.000		
76-	COUAD2	676	5	16	20	18	14	0.000		
77-	COUAD2	677	5	16	20	18	14	0.000		
78-	COUAD2	678	5	16	20	18	14	0.000		
79-	COUAD2	679	5	16	20	18	14	0.000		
80-	COUAD2	680	5	16	20	18	14	0.000		
81-	COUAD2	681	5	19	23	21	17	0.000		
82-	COUAD2	682	5	19	23	21	17	0.000		
83-	COUAD2	683	5	19	23	21	17	0.000		
84-	COUAD2	684	5	19	23	21	17	0.000		
85-	COUAD2	685	5	19	23	21	17	0.000		
86-	COUAD2	686	5	19	23	21	17	0.000		
87-	COUAD2	687	5	19	23	21	17	0.000		
88-	COUAD2	688	5	19	23	21	17	0.000		
89-	COUAD2	689	5	19	23	21	17	0.000		
90-	COUAD2	690	5	19	23	21	17	0.000		
91-	COUAD2	691	5	20	24	22	18	0.000		
92-	COUAD2	692	5	20	24	22	18	0.000		
93-	COUAD2	693	5	20	24	22	18	0.000		
94-	COUAD2	694	5	20	24	22	18	0.000		
95-	COUAD2	695	5	20	24	22	18	0.000		
96-	COUAD2	696	5	20	24	22	18	0.000		
97-	COUAD2	697	5	20	24	22	18	0.000		
98-	COUAD2	698	5	20	24	22	18	0.000		
99-	COUAD2	699	5	20	24	22	18	0.000		
100-	COUAD2	700	5	20	24	22	18	0.000		

```
CARD
COUNT      . 1 ..  2 ..  3 ..  4 ..  5 ..  6 ..  7 ..  8 ..  9 .
  101-     CQUAD2  701     5      23     27     25     21     0.000
  102-     CQUAD2  702     5      23     27     25     21     0.000
  103-     CQUAD2  703     5      23     27     25     21     0.000
  104-     CQUAD2  704     5      23     27     25     21     0.000
  105-     CQUAD2  705     5      23     27     25     21     0.000
  106-     CQUAD2  706     5      23     27     25     21     0.000
  107-     CQUAD2  707     5      23     27     25     21     0.000
  108-     CQUAD2  708     5      23     27     25     21     0.000
  109-     CQUAD2  709     5      23     27     25     21     0.000
  110-     CQUAD2  710     5      23     27     25     21     0.000
  111-     CQUAD2  711     5      24     28     26     22     0.000
  112-     CQUAD2  712     5      24     28     26     22     0.000
  113-     CQUAD2  713     5      24     28     26     22     0.000
  114-     CQUAD2  714     5      24     28     26     22     0.000
  115-     CQUAD2  715     5      24     28     26     22     0.000
  116-     CQUAD2  716     5      24     28     26     22     0.000
  117-     CQUAD2  717     5      24     28     26     22     0.000
  118-     CQUAD2  718     5      24     28     26     22     0.000
  119-     CQUAD2  719     5      24     28     26     22     0.000
  120-     CQUAD2  720     5      24     28     26     22     0.000
  121-     CROD    1       1      1      2
  122-     CROD    2       1      3      4
  123-     CROD    3       1      5      6
  124-     CROD    4       1      7      8
  125-     CROD    5       1      9      10
  126-     CROD    6       1      11     12
  127-     CROD    7       1      13     14
  128-     CROD    8       1      15     16
  129-     CROD    9       1      17     18
  130-     CROD    10      1      19     20
  131-     CROD    11      1      21     22
  132-     CROD    12      1      23     24
  133-     CROD    13      1      25     26
```

```
CARD
COUNT      . 1 ..  2 ..  3 ..  4 ..  5 ..  6 ..  7 ..  8 ..  9 .
 134-      CROD    14      1       27      28
 135-      CROD    15      2       1       5
 136-      CROD    16      2       2       6
 137-      CROD    17      2       3       7
 138-      CROD    18      2       4       8
 139-      CROD    19      2       5       9
 140-      CROD    20      2       6       10
 141-      CROD    21      2       7       11
 142-      CROD    22      2       8       12
 143-      CROD    23      2       9       13
 144-      CROD    24      2       10      14
 145-      CROD    25      2       11      15
 146-      CROD    26      2       12      16
 147-      CROD    27      2       13      17
 148-      CROD    28      2       14      18
 149-      CROD    29      2       15      19
 150-      CROD    30      2       16      20
 151-      CROD    31      2       17      21
 152-      CROD    32      2       18      22
 153-      CROD    33      2       19      23
 154-      CROD    34      2       20      24
 155-      CROD    35      2       21      25
 156-      CROD    36      2       22      26
 157-      CROD    37      2       23      27
 158-      CROD    38      2       24      28
 159-      CSHEAR  201     3       1       2       6       5
 160-      CSHEAR  202     3       5       6       10      9
 161-      CSHEAR  203     3       9       10      14      13
 162-      CSHEAR  204     3       13      14      18      17
 163-      CSHEAR  205     3       17      18      22      21
 164-      CSHEAR  206     3       21      22      26      25
 165-      CSHEAR  207     3       3       4       8       7
 166-      CSHEAR  208     3       7       8       12      11
```

```
CARD
COUNT      .  1  ..  2  ..  3  ..  4  ..  5  ..  6  ..  7  ..  8  ..  9  .
 167-      CSHEAR  209     3       11      12      16      15
 168-      CSHEAR  210     3       15      16      20      19
 169-      CSHEAR  211     3       19      20      24      23
 170-      CSHEAR  212     3       23      24      28      27
 171-      CSHEAR  213     4       1       2       4       3
 172-      CSHEAR  214     4       5       6       8       7
 173-      CSHEAR  215     4       9       10      12      11
 174-      CSHEAR  216     4       13      14      16      15
 175-      CSHEAR  217     4       17      18      20      19
 176-      CSHEAR  218     4       21      22      24      23
 177-      CSHEAR  219     4       25      26      28      27
 178-      FORCE   6       6       0       1.0     .0      .0      1.0
 179-      FORCE   7       7       0       1.0     .0      .0      1.0
 180-      FORCE   8       8       0       1.0     .0      .0      1.0
 181-      FORCE   11      11      0       1.0     .0      .0      1.0
 182-      FORCE   12      12      0       1.0     .0      .0      1.0
 183-      FORCE   15      15      0       1.0     .0      .0      1.0
 184-      FORCE   17      17      0       1.0     .0      .0      1.0
 185-      FORCE   18      18      0       1.0     .0      .0      1.0
 186-      FORCE   21      21      0       1.0     .0      .0      1.0
 187-      FORCE   23      23      0       1.0     .0      .0      1.0
 188-      FORCE   26      26      0       1.0     0.0     0.0     1.0
 189-      FORCE   27      27      0       1.0     0.0     0.0     1.0
 190-      PROSET                                                  6
 191-      GRID    1               0.000   0.000   2.000
 192-      GRID    2               0.000   0.000   -2.000
 193-      GRID    3               25.000  0.000   2.000
 194-      GRID    4               25.000  0.000   -2.000
 195-      GRID    5               0.000   30.000  2.000
 196-      GRID    6               0.000   30.000  -2.000
 197-      GRID    7               25.000  30.000  2.000
 198-      GRID    8               25.000  30.000  -2.000
 199-      GRID    9               0.000   60.000  2.000
 200-      GRID    10              0.000   60.000  -2.000
```

```
CARD
COUNT        .  1  ..  2  ..  3  ..  4  ..  5  ..  6  ..  7  ..  8  ..  9  .
  201-       GRID     11            25.000  60.000  2.000
  202-       GRID     12            25.000  60.000  -2.000
  203-       GRID     13            0.000   90.000  2.000
  204-       GRID     14            0.000   90.000  -2.000
  205-       GRID     15            25.000  90.000  2.000
  206-       GRID     16            25.000  90.000  -2.000
  207-       GRID     17            0.000   120.000 2.000
  208-       GRID     18            0.000   120.000 -2.000
  209-       GRID     19            25.000  120.000 2.000
  210-       GRID     20            25.000  120.000 -2.000
  211-       GRID     21            0.000   150.000 2.000
  212-       GRID     22            0.000   150.000 -2.000
  213-       GRID     23            25.000  150.000 2.000
  214-       GRID     24            25.000  150.000 -2.000
  215-       GRID     25            0.000   180.000 2.000
  216-       GRID     26            0.000   180.000 -2.000
  217-       GRID     27            25.000  180.000 2.000
  218-       GRID     28            25.000  180.000 -2.000
  219-       MAT1     1     10.5+6         .3      2.32-4
  220-       MAT2     2     21.55+5 3.3+5  .0      1.3+6   .0      .83+5
  221-       PQUAD2   3     1       .0025  .0
  222-       PQUAD2   6     2       .00025 .0
  223-       PROD     1     1       .01
  224-       PROD     2     1       2.0
  225-       PSHEAR   3     1       .05
  226-       PSHEAR   4     1       .04
  227-       SPC1     1     123456  1       THRU    4
             ENDDATA
```

```
      PROGRAM DIVERGE(INPUT,OUTPUT,DATA,TAPE5=DATA)
      DIMENSION A(12,12), ATINV(12,12), FLEX(12,12), FX(12,12), R(12)
     1         ,THETA1(12), THETA2(12), XCP(12), XV(12), Y(12), C(12)
     2         ,ENCM1(20),D(12,12)

      INTEGER P,Q
      REAL LAMBDA,MINF

C     ...INITIALIZE VARIABLES
      DATA J/02/,K/0./,LAMBDA/-00.00/,SPAN/100./,CORD/20./,
     1     MINF/0.00/,PI/3.1-1593/
      ANGLE=LA
      LAMBDA=LAMBDA*PI/180.
      P=SP/(2.*COS(LAMBDA))   ;   CT=CR=CORD/COS(LAMBDA)

      P=J*K
C     ...INITIALIZE THE FX,THETA1, AND THETA2 MATRICIES.
      DO 10 L=1,N
      THETA1(L)=1.0/(P+1-L)
      THETA2(L)=3.0
      DO 10 M=1,N
      FX(L,M)=0.0
   10 CONTINUE

C     ...CALCULATE THE WING 'E ELEMENT COORDINATES
      BETA=(1.0-MINF**2.0)**.5
      SN=P/(2.0*K)

      DO 200 I=1,K
      C(I)=((CT-CR)*(2.0*SN*(I-1)+SN)/3+CR)/BETA
      R(I)=C(I)/(2.0*J)
      Q=2*I-1
      Y(Q)=Y(Q+1)=2*SN*I
```

```
      XV(0)=Y(0)*TAN(LAMBDA)
      XV(0+1)=Y(0+1)*TAN(LAMBDA)+2*R(I)
      XCP(0)=XV(0)+R(I)
      XCP(0+1)=XV(0+1)+R(I)
  200 CONTINUE

C     ...CALCULATE THE MATRIX A(M,N)
      DO 210 M=1,P
      DO 210 N=1,P
      XBAR=XCP(M)-XV(N)
      YBAR=Y(M)-Y(N)
      A(M,N)=((((YBAR-SN)**2+XBAR**2)**.5+XBAR)/(YBAR-SN)-
     2       (((YBAR+SN)**2+XBAR**2)**.5+XBAR)/(YBAR+SN))
     3       /(XBAR*4.0*PI)
  210 CONTINUE

      PRINT*,"THE MATRIX A IS:"
      WRITE (10,((A(I,J),J=1,P),I=1,P)

C     ...INVERT THE MATRIX A(M,N)
      CALL MINV (A,AINV,P)

      PRINT*,"THE MATRIX AINV IS:"
      WRITE 410,((AINV(I,J),J=1,P),I=1,P)

C     ...READ IN THE DISPLACEMENT MATRIX.
      READ (5,400)((D(J,I),J=1,P),I=1,P)
  400 FORMAT (12(/,/,/,/,/,/,/,12(E9X,E13.6,/,/)))

      PRINT*,"THE D MATRIX IS:"
      WRITE 410,((D(I,J),J=1,P),I=1,P)

C     ...CONVERT THE DISPLACEMENT MATRIX TO THE FLEXIBILITY MATRIX
      DO 250 II=1,P
      DO 250 JJ=1,P,2
```

```
      FLEX(JJ,II)=FLEX(JJ+1,II)=(D(JJ,II)-D(JJ+1,II))/(2.*R(1))
  250 CONTINUE

      PRINT*,"THE FLEX MATRIX IS:"
      WRITE 410,((FLEX(I,J),J=1,P),I=1,P)

C     ...MULTIPLY THE FLEX MATRIX BY THE AINV MATRIX.
      DO 300 I=1,P
      DO 300 J=1,P
      DO 300 K=1,P
      FX(J,I)=FX(J,I)+FLEX(J,K)*AINV(K,I)
  300 CONTINUE

      PRINT *,"THE FX MATRIX IS:"
      WRITE 410,((FX(I,J),J=1,P),I=1,P)
  410 FORMAT ("0",2(1H ,5(E12.6,2X),/))

C     ...NOW USE STARDLAS METHOD TO CALCULATE THE EIGENVALUE LAMBDA.

C     ...BEGIN ITERATING UNTIL THE NORMALIZED THETA2 VECTOR
C        CONVERGES TO THETA1.
      DO 340 ITER =1,20

C     ...MULTIPLY FX BY THETA1.
      DO 310 J=1,P
      DO 310 K=1.P
      THETA2(J)=THETA2(J)+FX(J,K)*THETA1(K)
  310 CONTINUE

C     ...NORMALIZE  THETA2.
      TNORM(ITER)=ABS(THETA2(P))
      DO 320 J=1,P
      THETA2(J)=THETA2(J)/TNORM(ITER)
  320 CONTINUE
      PRINT *,"AFTER ITERATION NO. ",ITER
```

```
105                   PRINT *,"THE EIGENVALUE 1/LAMBDA IS ",INORM(ITER)
                      PRINT *,"THE EIGENVECTOR THETA IS:"
                      WRITE 420,(THETA2(J),J=1,P)
                  420 FORMAT (" ",3(" ",8(E12.6,2X),/))

110               C   ...CHECK FOR CONVERGENCE.
                      IF (ITER.EQ.1) GO TO 330
                      DIF=INORM(ITER)-INORM(ITER-1)
                      DIF=ABS(DIF)
                      PRINT*,"THE DIFFERENCE BETWEEN THIS INORM AND THE"
115                   PRINT*,"PREVIOUS INORM IS:  ",DIF
                      PRINT *," "
                      IF (DIF .LE. .000001) GO TO 500
                  330 CONTINUE
                  C   ...IF IT HAS NOT CONVERGED, GO TO THE NEXT ITERATION.
120                   DO 340 J=1,P
                      THETA1(J)=THETA2(J)
                      THETA2(J)=0.0
                  340 CONTINUE
                  350 CONTINUE
125                   PRINT*,"DID NOT CONVERGE"
                      GO TO 900
                  500 CONTINUE
                  C
                  C   ...NOW CALCULATE THE DIVERGENCE DYNAMIC PRESSURE AND
130               C      THE DIVERGENCE SPEED
                      QD=1.0/(INORM(ITER)**2*.5*SN)
                      UD=SQRT(144.0/(INORM(ITER)**2*0.0*.00236*SN))
                      WRITE 450
                  450 FORMAT ("1",5(/))
135                   PRINT*," FOR LAMBDA = ",ANGLE
                      PRINT*,"       SPAN = ",SPAN
                      PRINT*,"       CORD = ",CORD
                      PRINT*,"         SN = ",SN
                      PRINT*,"          R = ",R(1)
```

```
140               PRINT*," "
                  PRINT*,"**********************************************"
                  PRINT*," "
                  PRINT*,"THE DIVERGENCE DYNAMIC PRESSURE IS:  ",QD
                  PRINT*," "
145               PRINT*,"THE DIVERGENCE SPEED IS:  ",UD," FT PER SEC"
                  PRINT*," "
                  PRINT*,"**********************************************"

                  STOP "END OF DIVERG"
150               END
```

Vita

David C. Bannerman, born 4 May 1955, lived in Frankenmuth, Michigan for the first 18 years of his life. The next four years were spent at the University of Michigan, School of Engineering. He graduated with a Bachelor of Science degree in Aerospace Engineering in April of 1977. The same day he received his commission into the United States Air Force through the ROTC program. David then enrolled in the School of Engineering, Air Force Institute of Technology and began work on a Master's Degree in Aeronautical Engineering in October of the same year.

REPORT DOCUMENTATION PAGE

READ INSTRUCTIONS BEFORE COMPLETING FORM

1. REPORT NUMBER: AFIT/GAE/AA/78D-1	2. GOVT ACCESSION NO.
3. RECIPIENT'S CATALOG NUMBER	
4. TITLE (and Subtitle): A STUDY OF THE USE OF LAMINATED COMPOSITE WING STRUCTURES FOR CONTROLLING THE DIVERGENCE SPEED OF FORWARD SWEPT WINGS	5. TYPE OF REPORT & PERIOD COVERED: MS Thesis
	6. PERFORMING ORG. REPORT NUMBER
7. AUTHOR(s): David C. Bannerman, 2nd Lt USAF	8. CONTRACT OR GRANT NUMBER(s)
9. PERFORMING ORGANIZATION NAME AND ADDRESS: Air Force Institute of Technology (AFIT/ENY), Wright-Patterson AFB, Ohio 45433	10. PROGRAM ELEMENT, PROJECT, TASK AREA & WORK UNIT NUMBERS
11. CONTROLLING OFFICE NAME AND ADDRESS	12. REPORT DATE: December 1978
	13. NUMBER OF PAGES: 72
14. MONITORING AGENCY NAME & ADDRESS(if different from Controlling Office)	15. SECURITY CLASS. (of this report): UNCLASSIFIED
	15a. DECLASSIFICATION/DOWNGRADING SCHEDULE

16. DISTRIBUTION STATEMENT (of this Report)

Approved for public release; distribution unlimited.

17. DISTRIBUTION STATEMENT (of the abstract entered in Block 20, if different from Report)

18. SUPPLEMENTARY NOTES

Approved for public release;
IAW AFR 190-17

Joseph P. Hipps, Major, USAF
Director of Information

19. KEY WORDS (Continue on reverse side if necessary and identify by block number)

Forward Swept Wings
Composites
Static Stability
Wing Divergence

20. ABSTRACT (Continue on reverse side if necessary and identify by block number)

This thesis is an investigation of the effects of composite laminate orientation on the divergence problem of forward swept wings. The aerodynamic and structural properties are modeled with a doublet lattice technique and finite element method, respectively. The static equilibrium equation is applied to combine the two models. This results in an eigenvalue problem with the divergence dynamic pressure as the lowest eigenvalue.

A computer program is written to formulate and solve the eigenvalue problem. It is applied to two cases of example wings. For the first case, 100% of the

20(cont)
fibers are varied from 0° to 50° ahead of the structural swept axis for five different sweep angles. For the second case, only 70% of the fibers are varied while the remaining fibers are oriented at 90° and ± 45° to the structural sweep axis.

The results indicate that the divergence problem can be effectively controlled and possibly eliminated by properly orienting the composite laminates. The divergence speed was found to increase and reach a maximum as the principal fiber direction is swept forward. Maximum values occur for fibers oriented between 15° and 20° ahead of the structural swept axis for wing swept forward more than 25°.